
Universally Expressive Communication in Multi-Agent Reinforcement Learning

Matthew Morris

InstaDeep Ltd.

m.morris@instadeep.com

Thomas D. Barrett

InstaDeep Ltd.

t.barrett@instadeep.com

Arnu Pretorius

InstaDeep Ltd.

a.pretorius@instadeep.com

Abstract

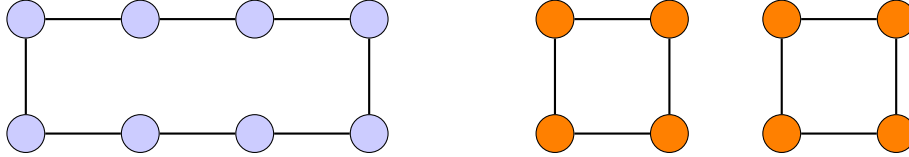
Allowing agents to share information through communication is crucial for solving complex tasks in multi-agent reinforcement learning. In this work, we consider the question of whether a given communication protocol can express an arbitrary policy. By observing that many existing protocols can be viewed as instances of graph neural networks (GNNs), we demonstrate the equivalence of joint action selection to node labelling. With standard GNN approaches provably limited in their expressive capacity, we draw from existing GNN literature and consider augmenting agent observations with: (1) unique agent IDs and (2) random noise. We provide a theoretical analysis as to how these approaches yield universally expressive communication, and also prove them capable of targeting arbitrary sets of actions for identical agents. Empirically, these augmentations are found to improve performance on tasks where expressive communication is required, whilst, in general, the optimal communication protocol is found to be task-dependent.

1 Introduction

Communication lies at the heart of many multi-agent reinforcement learning (MARL) systems. In MARL, multiple agents must account for each other’s actions during both training and execution and, indeed, solving complex tasks in high-dimensional spaces often requires a cooperative joint policy that is difficult, or even impossible, to learn independently. Therefore, allowing agents to share information is crucial and how best to achieve this has remained a keen area of research since the seminal proposals of learned communication by Foerster et al. [14] and Sukhbaatar et al. [51]. Whilst no single universally-adopted approach has emerged, considerations for MARL communication include inductive biases that aid learning. For example, an agent’s policy should often not depend on the order in which messages are received at a given time step. i.e. be *permutation invariant*.

In this context, graph neural networks (GNNs) provide a rich framework for MARL communication. It is natural to consider agents as nodes in a graph, with communication channels corresponding to edges between them. GNNs are specifically designed to respect this (typically non-Euclidian) structure [5] and, indeed, many of the most successful MARL communication models fall within this paradigm, including CommNet [51], IC3Net [49], GA-Comm [29], MAGIC [37], Agent-Entity Graph [2], IP [44], TARMAC [9], IMMAC [52], DGN [24], VBC [64], MAGNet [33], and TMC [65]. However, although traditional GNNs – such as those used in MARL to date – can readily provide permutation invariant communication, they are not universally expressive.

Figure 1: A pair of graphs indistinguishable by 1-WL



The expressivity of GNNs is often considered in the context of the 1-WL graph coloring algorithm [60]. In brief, 1-WL tests if two graphs are non-isomorphic by iteratively re-coloring the nodes and has been proven to *not* be universally expressive (i.e. there exist non-isomorphic graphs that 1-WL can't distinguish). Moreover, Morris et al. [34] and Xu et al. [61] proved that for any two non-isomorphic graphs indistinguishable by 1-WL, there is no GNN that can produce different outputs for those two graphs. An example of such graphs is given in Figure 1. This direct correspondence between GNNs and 1-WL equivalently limits the expressivity of any MARL communication built on top of GNNs. Whilst higher-order GNN architectures which go beyond 1-WL expressivity have been proposed (see [35] for an overview), many of these models do not scale well and are computationally infeasible in practice. However, recent works have shown that augmenting the node features can provide an alternative path to increased expressivity without computationally expensive architectural changes [1, 10]. It is then natural to ask if, and how, these advancements can be brought into the MARL setting.

In this paper, we investigate the effectiveness of GNNs for universally expressive communication in MARL. We define *Graph Decision Networks* (GDNs), a framework for MARL communication which captures many of the most successful methods. We highlight the correspondence between GDNs and the node labeling problem in GNNs, thus making concrete the limits of GDN expressivity. For moving beyond these limits, we consider two augmentations from the GNN literature – random node initialization (RNI) [1] and colored local iterative procedure (CLIP) [10], where random noise and unique labels are added to graph nodes, respectively. We provide a theoretical analysis as to how these algorithms yield universally expressive communication in MARL, and also prove their ability to solve coordination problems where the optimal policy requires arbitrary sets of actions from identical agents. We then perform an empirical study where we augment several state-of-the-art MARL communication algorithms with RNI and unique labels. By evaluating performance across both standard benchmarks and specifically designed tasks, we show that when complex non-local coordination or symmetry breaking is required, universally expressive communication can provide significant performance improvements. However, in more moderate cases, augmented communication can reduce convergence speeds and result in suboptimal policies. Therefore, whilst more expressive GNN architectures are required to improve performance on certain problems, a more complete picture relating expressivity to downstream performance remains an open question for future work.

2 Background

Multi-Agent Reinforcement Learning We consider the setting of Decentralized Partially Observable Markov Decision Processes [39] augmented with communication between agents. At each timestep t every agent $i \in \{1, \dots, N\}$ gets a local observation o_i^t , takes an action a_i^t , and receives a reward r_i^t . We consider two agent paradigms: value-based [53] and actor-critic [15, 32]. For brevity, we collectively refer to the policy network in actor-critic methods and the Q-network in value-based methods as the *actor network*. In this paper, we consider by default parameter sharing between agent's networks, which is often used to yield faster and more stable training in MARL [14, 18, 45, 62].

Graph Neural Networks GNNs can refer to a large variety of models; in this paper, we define the term to correspond to the definition of Message Passing Neural Networks (MPNNs) by Gilmer et al. [17], which is the most common GNN architecture. Notable instances of this architecture include Graph Convolutional Networks (GCNs) [12], GraphSAGE [19], and Graph Attention Networks (GATs) [56]. A GNN consists of multiple message-passing layers, each of which updates the node attributes / labels (terms used interchangeably). For layer m and node i with current attribute v_i^m , the new attribute v_i^{m+1} is computed as

$$v_i^{m+1} := f_{\text{update}}^{\theta_m}(v_i^m, f_{\text{aggr}}^{\theta'_m}(\{v_j^m \mid j \in N(i)\}), f_{\text{read}}^{\theta''_m}(\{v_j^m \mid j \in V(G)\}))$$

where $N(i)$ is all nodes with edges connecting to i and $\theta_m, \theta'_m, \theta''_m$ are the (possibly trainable) parameters of the update, aggregation, and readout functions for layer m . Parameters may be shared between layers, e.g. $\theta_0 = \theta_1$. The functions $f_{\text{aggr}}^{\theta'_m}, f_{\text{read}}^{\theta''_m}$ are permutation invariant. Importantly, GNNs are invariant / equivariant graph functions.

3 Expressivity of Multi-Agent Communication

3.1 Graph Decision Networks

Many of the most successful MARL communication methods can be captured within the following framework. At each time step, define an attributed graph $G = (V, E, a)$ with nodes $V(G) := \{\text{all agents}\}$, edges $E(G) := \{(i, j) \mid \text{agent } i \text{ is communicating with } j\}$, and for all agents i , the node i is labeled with the observation of i . This graph is passed through a GNN f which outputs values for each node and passes each resulting node value through the actor network of the corresponding agent. Assuming that the actor networks use shared weights, we can substitute them for a final GNN layer M , where $f_{\text{update}}^{\theta_M}(v, \sim) := P(v)$ and P represents the shared actor network. We refer to communication methods that fall within this paradigm as *graph decision networks* (GDNs).

Given the above assumption of shared weights, any GDN simply reduces to a GNN node labelling problem, where the correct label for a given node is the corresponding actor network output that collectively maximizes the joint reward (or the individual reward, depending on how the agent is trained). Going forward, we only deal with such GDNs (ones with a shared actor network). In the case of stochastic policies [15, 63], the target labels are parameters of output distributions, instead of atomic actions. This applies to both discrete and continuous distributions. Note that this is not how RL agents are actually trained (i.e. they use reward signals, not supervised learning).

However, given that this paper aims to analyze expressivity, we argue that it does not matter how the GDN is trained. All that expressivity is concerned with is the *ability* of a model to produce a certain output, not how the training paradigm causes the model to converge to the solution. All we have to know is that there are “optimal” actor network outputs for each agent, under some metric of optimality, and then we can reason about the ability of the model to provide these outputs. Scenarios with heterogeneous agents can still be considered within this paradigm, by allocating a portion of the observations to indicate the agent type (e.g. through a one-hot encoding) [54]. Models with recurrent networks also fall within the paradigm, where the hidden or cell states for the networks can be considered as part of the agent observations.

Due to the reduction of GDNs to a GNN node labelling problem, GDNs suffer from the same expressivity limits as GNNs, about which there is a plethora of work [4, 8, 16, 30, 31, 34, 38, 40, 61]. These are expanded upon in Appendix A.4. For our analysis, we focus particularly on ways to achieve universal Weisfeiler-Lehman expressivity, but note that the above reduction unlocks many tools for reasoning about the expressivity of GDNs.

3.2 Desired Properties of MARL Communication

Whilst conventional GDNs cannot capture functions with expressive power beyond 1-WL [34, 61], recent GNN architectures have been proposed to achieve expressivity beyond 1-WL, even ones which are able to express any equivariant graph function. We can use these insights to construct more expressive GDNs. However, we note that classes of models which always yield equivariant functions are not necessarily desirable, since they cannot break symmetries between agents when required. Many MARL environments require agents to coordinate, needing some joint action to solve the task. However, if agents have identical observations and communication graph structure in a pure GDN framework, there is no way for them to disambiguate between each other and distribute the required actions amongst themselves. For a simple example, consider a setting where two agents have identical observations but must take opposite actions – then the only way for them to solve the environment is to communicate in such a way that they can break this symmetry and take different actions from one another.

More formally, since GNNs are equivariant graph functions, GDNs are equivariant functions on the agent observations and communication graph structure. This means that agents within the same *graph orbit* will always produce the same output. For a graph G , consider two nodes $u, v \in G$. If there exists an automorphism α of G such that $\alpha(u) = v$, then u and v are said to be *similar nodes*. The relation *is similar to* forms an equivalence relation on the nodes of G . Each equivalence class is called an *orbit*. Intuitively, every node in an orbit “has the same structure”. We denote the set of all orbits of G by $R(G)$: this forms a partition of $V(G)$.

Theorem 1. *Given a GDN f , observations $O = \{o_1, \dots, o_n\}$, and communication graph G such that nodes i and j are similar in G and $o_i = o_j$, then it holds that $f(O)_i = f(O)_j$.*

Full proofs for all theorems in this paper can be found in Appendix B. We formally state the desired behaviour of GDNs – which we refer to as *symmetry breaking* – that would enable them to solve such coordination problems. Given a graph G with orbits $R(G)$, a GDN g ought to be able to produce, or *target*, a set of labels A_k for each orbit r_k :

$$\forall r_k \in R(G), \{g(G)_i \mid i \in r_k\} = A_k,$$

where $g(G)_i$ is the output of $g(G)$ for agent i . Thus, ideally, MARL communication methods should possess all the following properties: (1) universal expressivity for equivariant graph functions, (2) symmetry breaking for coordination problems, and (3) computational efficiency. We apply two existing GNN augmentations to GDNs to achieve this, both of which come with minimal extra computational cost.

3.3 Expressive Graph Decision Networks

Random Node Initialization Sato et al. [47] propose augmenting GNNs with *random node initialization* (RNI), where for each node in the input graph, a number of randomly sampled values are concatenated to the original node attribute. For all graphs / nodes, the random values are sampled from the same distribution. Abboud et al. [1] prove that such GNNs are universal and can approximate any permutation invariant / equivariant graph function. Technically, random initialization breaks the node invariance in GNNs, since the result of the message passing will depend on the structure of the graph as well as the values of the random initializations. However, when one views the model as computing a random variable, the random variable is still invariant when using RNI. In expectation, the mean of random features will be used for GNN predictions, and is the same across each node. However, the variability of the random samples allows the GNN to discriminate between nodes that have different random initializations, breaking the 1-WL upper bound.

Abboud et al. [1] formally state and prove a universal approximation result for invariant graph functions. They note that it can be extended to equivariant functions, which is what GDNs are. As such, we adapt and state the theorem for equivariant functions. Let G_n be the class of all n -node graphs. Let $f : G_n \rightarrow \mathbb{R}^n$, a graph function which outputs a real value for each node in $V(G)$. We say that a randomized function X that associates with every graph $G \in G_n$ a sequence of random variables $X_1(G), X_2(G), \dots, X_n(G)$, one for each node, is an (ϵ, δ) -approximation of f if for all $G \in G_n$ it holds that $\forall i \in \{1, 2, \dots, n\}, \Pr(|f(G)_i - X_i(G)| \leq \epsilon) \geq 1 - \delta$, where $f(G)_i$ is the output of $f(G)$ for node i . Note that a GNN h with RNI computes such functions X . If X is computed by h , we say that h (ϵ, δ) -approximates f . We can now state the following theorem:

Theorem 2. *Let $n \geq 1$ and let $f : G_n \rightarrow \mathbb{R}^n$ be equivariant. Then for all $\epsilon, \delta > 0$, there is a GNN with RNI that (ϵ, δ) -approximates f .*

Such GNNs are also able to solve symmetry-breaking coordination problems by using RNI to disambiguate between otherwise identical agents. To formally state this property, we need to define (ϵ, δ) -approximation for sets. We say that two sets A, B containing random variables are (ϵ, δ) -equal, denoted $A \cong_{\epsilon, \delta} B$, if there exists a bijection $\tau : A \rightarrow B$ such that $\forall a \in A, \Pr(|a - \tau(a)| \leq \epsilon) \geq 1 - \delta$.

Theorem 3. *Let $n \geq 1$ and consider a set T , where each $(G, A) \in T$ is a graph-labels pair, such that $G \in G_n$ and there is a set of target labels $A_k \in A$ for each orbit $r_k \in R(G)$, with $|A_k| = |r_k|$. Then for all $\epsilon, \delta > 0$ there is a GNN with RNI g which satisfies:*

$$\forall (G, A) \in T \quad \forall r_k \in R(G), \{g(G)_i \mid i \in r_k\} \cong_{\epsilon, \delta} A_k$$

Table 1: Architecture of the Baselines

Name	Communication Graph	Agents	GNN Architecture
CommNet [51]	Complete (or environment-based)	Recurrent A2C	Sum Aggregation
IC3Net [49]	Complete + Gating	Recurrent A2C	Sum Aggregation
TarMAC [9]	Complete + Learned Soft Edges	Recurrent A2C	GAT
T-IC3Net [49, 9]	Gating + Learned Soft Edges	Recurrent A2C	GAT
MAGIC [37]	Learned	Recurrent A2C	GAT
DGN [24]	Environment-based	Q-network	GCN

In the GDN case, adding RNI means concatenating noise to the agent observations, thus achieving universal approximation and enabling the solving of symmetry-breaking coordination problems.

Unique Node Identifiers Dasoulas et al. [10] augment GNNs with a coloring scheme to define *colored local iterative procedure* (CLIP). They use colors to differentiate otherwise identical node attributes, with k -CLIP corresponding to k different colorings being sampled and maximized over. They prove theoretically that when maximizing over all such possible colorings, ∞ -CLIP can represent any invariant graph function.

Assigning nodes unique IDs is equivalent to 1-CLIP, since this guarantees that every node with identical attributes will have a unique “color”: its particular unique ID. Therefore, we can leverage the universality result for 1-CLIP (Theorem 4 in [10]), which states that with any given degree of precision, 1-CLIP can approximate any invariant graph function. However, Dasoulas et al. [10] note that such solutions may be difficult to converge to and require a large number of training steps in practice. Intuitively, this is because the GNN has to learn to deal with $n!$ permutations of unique IDs. Similarly to the RNI case, we extend their theorem to equivariant functions.

Theorem 4. *Let $n \geq 1$ and let $f : G_n \rightarrow \mathbb{R}^n$ be equivariant. Then for all $\epsilon > 0$, there is a GNN with unique node IDs that ϵ -approximates f .*

Such GNNs can also solve symmetry-breaking coordination problems, in a similar way to ones with RNI. We say that two sets A, B , which do not contain random variables, are ϵ -equal, denoted $A \cong_\epsilon B$, if there exists a bijection $\tau : A \rightarrow B$ such that $\forall a \in A, |a - \tau(a)| \leq \epsilon$.

Theorem 5. *Let $n \geq 1$ and consider a set T , where each $(G, A) \in T$ is a graph-labels pair, such that $G \in G_n$ and there is a set of target labels $A_k \in A$ for each orbit $r_k \in R(G)$, with $|A_k| = |r_k|$. Then for all $\epsilon > 0$ there is a GNN with unique node IDs g which satisfies:*

$$\forall (G, A) \in T \quad \forall r_k \in R(G), \{g(G)_i \mid i \in r_k\} \cong_\epsilon A_k$$

In the GDN case, this means that by giving each agent a unique ID in its observations, we can achieve universal approximation and enabling the solving of symmetry-breaking coordination problems.

4 Experiments

4.1 Methods

Baselines For evaluation, we adopt a diverse selection of MARL communication methods which fall under the GDN paradigm. These are shown in Table 1, along with the communication graph structure, agent model, and GNN architecture. We use the code provided by Jiang et al. [24], Niu et al. [37] as starting points. All of the implementations are extended to support multiple rounds of message-passing and the baselines are augmented with the ability for their communication to be masked by the environment (e.g. based on distance or obstacles in the environment). We fix the number of message-passing rounds to be 4 and otherwise use the original models and hyperparameters from [24, 37]. Full experiment and hyperparameter details can be found in Appendix C, and full results are shown in Appendix D.

Environments **Predator-Prey** [9, 27, 29, 37, 49] and **Traffic Junction** [9, 27, 29, 37, 49, 51] are common MARL communication benchmarks. In Predator-Prey, predator agents are tasked with

capturing prey and in Traffic Junction, agents need to successfully navigate a traffic intersection (full descriptions of each environment are given in Appendix C.2). We perform evaluations on these benchmarks to test how well our universally expressive GDN models perform when there is not necessarily a benefit to having communication expressivity beyond 1-WL. We also introduce two new environments, Drone Scatter and Box Pushing, to respectively test symmetry-breaking and communication expressivity beyond 1-WL.

Drone Scatter consists of 4 drones in a homogeneous field surrounded by a fence. Their goal is to move around and find a target hidden in the field, which they can only notice when they get close to. The drones do not have GPS and can only see directly beneath them using their cameras, as well as observing their last action. The best way for them to locate the target is to split up and search in different portions of the field, despite them all having the same observations; thus, they are given rewards for splitting up.

Box Pushing consists of 10 robots in a 12x12 construction site, which has boxes within that need to be moved to the edge of the site: the clearing area. Robots attach themselves to boxes before they can move them; when attached, robots can no longer see around themselves. Free-roaming robots can communicate with any other free-roaming robots, but attached robots can only communicate with the robots directly adjacent to them. The environment either spawns with one large box or two small boxes and agents spawn already attached. 4 attached robots all moving in the same direction are needed to move a small box, and 8 all power moving in the same direction to move a large box. To solve the environment, the robots need to be able to communicate with each other to figure out which type of box they are on and all push correctly, at the same time, and in the same direction. Since the communication graphs corresponding to the scenarios with small and large boxes are 1-WL indistinguishable, communication beyond 1-WL is needed to optimally solve the environment.

Evaluation Procedure We augment baseline communication methods with RNI and unique IDs to perform our evaluations. Agent IDs are represented by one-hot encodings and “0.25 RNI” refers to 25% of the observation space being randomly initialized. We sample each RNI value uniformly from $[-1, 1]$. For each scenario and for every baseline communication method, we compare 4 models: the baseline without modifications, the baseline augmented with unique IDs for each agent, the baseline augmented with 0.75 RNI, and finally 0.25 RNI. The only exceptions are the Drone Scatter evaluations, where 0.25 RNI is not used since the observation space is not large enough, and the Drone Scatter experiments using stochastic evaluation, where DGN is not used since it does not support stochastic evaluation.

For each run, corresponding to a random initialization (one seed) of the model in question, we perform periodic evaluations during training. Each epoch consists of 5000 training episodes, after which 100 evaluation episodes are used to report aggregate metric scores, yielding an evaluation score for the model after every epoch. Following an established practice in MARL evaluation [15, 22, 41, 46, 59, 63, 66], we take the value of a metric for a run to be the *best* value achieved during training, so that our metrics are robust against runs which converge at some point and then degrade in performance as they continue to train. In such cases, one would use the parameters from the best performing model found during training for real-world evaluation; thus, that performance makes more sense to report than the model performance once training has finished. We utilize 10 seeds for Box Pushing experiments and 5 for all others. For each scenario, metric, baseline communication method, and variant thereof, we report the mean metric value across all seeds and a 95% confidence interval. To calculate the confidence interval, we assume a normal distribution and compute the interval as $1.96 \times \text{SEM}$ (standard error of the mean). Finally, for all Box Pushing experiments, we make use of a form of hybrid imitation learning to help deal with exceptionally sparse rewards (full details are given in Appendix C.3).

4.2 Results

Benchmark Environments Experimental results on the benchmark environments are shown in Table 2 for Easy Traffic Junction, Table 3 for Predator-Prey, and Table 4 for Medium Traffic Junction. In general, unique IDs tends to perform comparably to the baseline. The only exception to this is for IC3Net on Medium Traffic Junction, where unique IDs struggle.

0.75 RNI is categorically the worst method, consistently getting outperformed by all other methods and only coming out on top for MAGIC on Medium Traffic Junction, which is not significant due to

Table 2: Mean and 95% confidence interval for Easy Traffic Junction across all baselines

Baseline	Metric	Baseline	Unique IDs	0.75 RNI	0.25 RNI
CommNet	Success	1 ± 0	1 ± 0	1 ± 0	1 ± 0
DGN	Success	0.987 ± 0	0.99 ± 0	0.848 ± 0.15	0.996 ± 0
IC3Net	Success	1 ± 0	1 ± 0	1 ± 0	0.986 ± 0.02
MAGIC	Success	0.634 ± 0.11	0.764 ± 0.13	0.684 ± 0.11	0.787 ± 0.09
TarMAC	Success	0.994 ± 0.01	1 ± 0	0.933 ± 0.04	1 ± 0
T-IC3Net	Success	1 ± 0	0.998 ± 0	0.94 ± 0.04	0.974 ± 0.04

Table 3: Mean and 95% confidence interval for Predator-Prey across all baselines

Baseline	Metric	Baseline	Unique IDs	0.75 RNI	0.25 RNI
CommNet	Success	0.88 ± 0.03	0.908 ± 0.02	0.194 ± 0.02	0.476 ± 0.05
DGN	Success	0.014 ± 0	0.016 ± 0	0.026 ± 0.03	0.032 ± 0.01
IC3Net	Success	0.952 ± 0	0.93 ± 0.02	0.454 ± 0.08	0.933 ± 0.02
MAGIC	Success	0.892 ± 0.02	0.888 ± 0.05	0.112 ± 0.03	0.451 ± 0.09
TarMAC	Success	0.169 ± 0.09	0.24 ± 0.11	0.068 ± 0.01	0.086 ± 0.02
T-IC3Net	Success	0.938 ± 0.02	0.938 ± 0.01	0.27 ± 0.02	0.913 ± 0.02

the instability of that set of results. 75% of observations being randomly initialized appears far too much for the system to be able to learn effective policies. However, universality results still hold for lower ratios of RNI.

0.25 RNI exhibits strong performance on Easy Traffic Junction, always solving the environment and almost always outperforming the baseline. However, on sparse-reward problems (such as Predator-Prey and, to a lesser extent, Medium Traffic Junction) RNI methods typically take longer to converge than the baseline and unique IDs, and 0.25 RNI can struggle to reach the performance of baseline methods. This aligns with Abboud et al. [1]’s observation that GNNs with RNI take significantly longer to converge than normal GNNs. This is only exacerbated in a MARL setting with sparse reward signals, where slow convergence is expected regardless of the RNI augmentation. Indeed, on all examples, RNI methods typically take longer to converge than the baselines and unique IDs.

Overall, we conclude that both unique IDs and 0.25 RNI achieve sufficient performance on the benchmarks to qualify them for use, especially given that the extra expressivity they provide is not strictly necessary. With respect to the different baselines, we note that simple baselines such as CommNet work the best when the optimal policy is also simple, such as for Easy Traffic Junction, but that more sophisticated baselines outperform them on the complex environments. We also note the very unstable performance of MAGIC for the Traffic Junction environments.

Weisfeiler-Lehman Expressivity Results for the Box Pushing environment are shown in Table 5. 0.25 RNI is the clear winner, achieving the top performance across almost all baselines and only slightly worse performance in the others. It is never outperformed by the baseline. This indicates that when communication expressivity beyond 1-WL is helpful for solving the environment, using RNI is the clear choice. Across all but one method, unique IDs also outperformed the baseline, demonstrating the benefit of having higher expressivity. However, unique IDs tend to yield less stable solutions and less effective policies than 0.25 RNI.

Table 4: Mean and 95% confidence interval for Medium Traffic Junction across all baselines

Baseline	Metric	Baseline	Unique IDs	0.75 RNI	0.25 RNI
CommNet	Success	0.761 ± 0.31	0.793 ± 0.33	0.046 ± 0	0.614 ± 0.11
DGN	Success	1 ± 0	1 ± 0	0.062 ± 0	0.619 ± 0.4
IC3Net	Success	0.971 ± 0.04	0.804 ± 0.1	0.588 ± 0.03	0.855 ± 0.13
MAGIC	Success	0.551 ± 0.28	0.526 ± 0.33	0.734 ± 0.21	0.4 ± 0.35
TarMAC	Success	0.064 ± 0	0.052 ± 0	0.05 ± 0	0.054 ± 0.01
T-IC3Net	Success	0.89 ± 0.17	0.909 ± 0.08	0.362 ± 0.18	0.962 ± 0.02

Table 5: Mean and 95% confidence interval for Box Pushing across all baselines

Baseline	Metric	Baseline	Unique IDs	0.75 RNI	0.25 RNI
CommNet	Ratio Cleared	0.786 ± 0.08	0.829 ± 0.08	0.768 ± 0.08	0.795 ± 0.09
DGN	Ratio Cleared	0.603 ± 0	0.756 ± 0.06	0.958 ± 0	0.957 ± 0.01
IC3Net	Ratio Cleared	0.49 ± 0.15	0.617 ± 0.14	0.34 ± 0.18	0.676 ± 0.06
MAGIC	Ratio Cleared	0.958 ± 0.04	0.985 ± 0.01	0.975 ± 0.04	0.998 ± 0
TarMAC	Ratio Cleared	0.629 ± 0.14	0.578 ± 0.11	0.662 ± 0.06	0.679 ± 0.06
T-IC3Net	Ratio Cleared	0.558 ± 0.13	0.596 ± 0.11	0.458 ± 0.18	0.643 ± 0.15

Table 6: Mean and 95% confidence interval for Drone Scatter across all baselines except DGN, including a purely random agent. Stochastic evaluation

Baseline	Metric	Baseline	Unique IDs	0.75 RNI
CommNet	Pairwise Distance	11.34 ± 0.9	12.08 ± 1.12	8.687 ± 1.4
	Steps Taken	11.5 ± 0.26	9.767 ± 0.32	11.74 ± 1.39
IC3Net	Pairwise Distance	9.108 ± 1.45	13.3 ± 0.71	10.99 ± 0.38
	Steps Taken	11.94 ± 0.84	10.13 ± 0.25	11.66 ± 0.22
MAGIC	Pairwise Distance	7.693 ± 1.47	12.59 ± 1	7.216 ± 0.76
	Steps Taken	13.05 ± 0.58	11.12 ± 1.05	13.54 ± 0.21
TarMAC	Pairwise Distance	7.448 ± 0.89	10.26 ± 0.69	8.486 ± 0.36
	Steps Taken	13.49 ± 0.1	10.7 ± 0.35	12.85 ± 0.57
T-IC3Net	Pairwise Distance	8.891 ± 0.27	12.9 ± 0.78	9.552 ± 0.57
	Steps Taken	12.28 ± 0.6	10.33 ± 0.46	12.22 ± 0.82
Random	Pairwise Distance	5.8 ± 0.02	—	—
	Steps Taken	17.39 ± 0.04	—	—

For completeness, we note that expressivity beyond 1-WL is not strictly needed to solve the Box Pushing environment, as demonstrated by several baselines achieving a “ratio cleared” score greater than 0.5, meaning they learned to sometimes clear both types of boxes. This is because the environment can be solved, albeit inefficiently, by recurrent policies which learn to alternate actions between “normal” and “power” moves each time step. Such policies are guaranteed to move the box every 2 time steps.

Symmetry Breaking Results for the Drone Scatter experiments are shown in Table 6 and Table 7, for agents with stochastic and greedy evaluation respectively. Across all of them, unique IDs exhibits consistently superior performance than 0.75 RNI and the baseline, since it deterministically breaks the symmetry between agents and allows them to split up easily to solve the environment. In the stochastic case, 0.75 RNI performs similarly to the baseline, but is markedly superior to the baseline in the greedy case. The comparison to a purely random agent indicates that the models are learning much more effective policies than just moving around at random.

Baseline methods with stochastic evaluation achieve consistently higher pairwise distances than their greedy counterparts, meaning they are learning to split up to find the target. They are capable of this due to a combination of 3 things: a stochastic policy, recurrent networks, and agents observing their last actions. Initially, agents cannot differentiate between each other, and all produce the same action distribution. However, if the distribution is diverse, then they are expected to produce different actions since they sample randomly from this distribution, which are observed in the next time step. The different observations lead to different hidden states in the recurrent networks, effectively changing the observations between agents and allowing them to differentiate between each other. This is not the case for greedy action selection, which is common when doing policy evaluation in MARL, where the actions chosen will always be the same.

5 Conclusion

We introduce GDNs, a framework for MARL communication, and formally show how it corresponds to the node labelling problem in GNNs. Our theoretical contributions use this observation to demonstrate that existing MARL communication methods relying on conventional GNN architectures

Table 7: Mean and 95% confidence interval for Drone Scatter across all baselines. Greedy evaluation

Baseline	Metric	Baseline	Unique IDs	0.75 RNI
CommNet	Pairwise Distance	8.849 \pm 0.63	13.28 \pm 1.27	8.589 \pm 1.35
	Steps Taken	13.79 \pm 0.12	9.554 \pm 0.33	12.62 \pm 1.19
DGN	Pairwise Distance	3.221 \pm 0.18	4.427 \pm 0.67	3.706 \pm 0.83
	Steps Taken	13.36 \pm 0.15	13.27 \pm 0.21	13.46 \pm 0.14
IC3Net	Pairwise Distance	7.69 \pm 1.03	14.09 \pm 0.54	11 \pm 0.86
	Steps Taken	13.25 \pm 0.4	10.14 \pm 0.2	11.42 \pm 0.48
MAGIC	Pairwise Distance	6.61 \pm 1.28	12.58 \pm 0.6	7.107 \pm 1.59
	Steps Taken	13.27 \pm 0.18	11.84 \pm 0.68	13.61 \pm 0.25
TarMAC	Pairwise Distance	8.666 \pm 0.28	12.09 \pm 0.73	8.999 \pm 0.94
	Steps Taken	13.73 \pm 0.21	11.01 \pm 0.86	12.19 \pm 0.82
T-IC3Net	Pairwise Distance	7.28 \pm 0.69	13.51 \pm 0.98	10.87 \pm 1.17
	Steps Taken	13.96 \pm 0.26	10.63 \pm 0.66	11.73 \pm 0.54

have provably limited expressivity. Driven by this, we prove how augmenting agent observations with unique IDs or random noise yields universally expressive invariant communication in MARL, whilst also providing desirable properties such as being able to perform symmetry-breaking: targeting arbitrary sets of joint actions for identical agents.

Experimentally, we compare these augmentations across 6 different MARL communication baselines that fall within the GDN paradigm, using 3 benchmark communication environments and 2 tasks designed to separately test expressivity and symmetry-breaking. Ultimately, we find that, whilst unique IDs or smaller RNI augmentations can typically be applied without detriment on standard environments, they do not readily provide improved performance either. However, on environments where more complex coordination is required, these augmentations are essential for strong performance. With RNI and unique IDs being best suited to environments requiring increased expressivity and symmetry-breaking, respectively, it is interesting to note that no single method emerges which we can recommend as the *de facto* choice for MARL practitioners. This suggests that a more complete picture of the relationship between communication expressivity and downstream performance on relevant tasks remains an open question for future research. Furthermore, insights into GNN architectures can be leveraged in GDNs, which opens many promising avenues for future work in MARL communication.

References

- [1] Ralph Abboud, Ismail Ilkan Ceylan, Martin Grohe, and Thomas Lukasiewicz. The surprising power of graph neural networks with random node initialization. *Proceedings of the 30th International Joint Conference on Artificial Intelligence (IJCAI)*, pages 2112–2118, 2021.
- [2] Akshat Agarwal, Sumit Kumar, and Katia Sycara. Learning transferable cooperative behavior in multi-agent teams. *arXiv preprint arXiv:1906.01202*, 2019.
- [3] Albert-Laszlo Barabasi and Zoltan N Oltvai. Network biology: understanding the cell’s functional organization. *Nature reviews genetics*, 5(2):101–113, 2004.
- [4] Pablo Barceló, Egor Kostylev, Mikael Monet, Jorge Pérez, Juan Reutter, and Juan-Pablo Silva. The logical expressiveness of graph neural networks. In *8th International Conference on Learning Representations (ICLR 2020)*, 2020.
- [5] Michael M Bronstein, Joan Bruna, Taco Cohen, and Petar Veličković. Geometric deep learning: Grids, groups, graphs, geodesics, and gauges. *arXiv preprint arXiv:2104.13478*, 2021.
- [6] Jacopo Castellini, Frans A Oliehoek, Rahul Savani, and Shimon Whiteson. The representational capacity of action-value networks for multi-agent reinforcement learning. *18th International Conference on Autonomous Agents and Multiagent Systems*, 2019.
- [7] Zhengdao Chen, Soledad Villar, Lei Chen, and Joan Bruna. On the equivalence between graph isomorphism testing and function approximation with gnns. *Advances in neural information processing systems*, 32, 2019.
- [8] Zhengdao Chen, Lei Chen, Soledad Villar, and Joan Bruna. Can graph neural networks count substructures? *Advances in neural information processing systems*, 33:10383–10395, 2020.
- [9] Abhishek Das, Théophile Gervet, Joshua Romoff, Dhruv Batra, Devi Parikh, Mike Rabbat, and Joelle Pineau. Tarmac: Targeted multi-agent communication. In *International Conference on Machine Learning*, pages 1538–1546. PMLR, 2019.
- [10] George Dasoulas, Ludovic Dos Santos, Kevin Scaman, and Aladin Virmaux. Coloring graph neural networks for node disambiguation. *International Joint Conference on Artificial Intelligence*, pages 2126–2132, 2020.
- [11] Kefan Dong, Yuping Luo, Tianhe Yu, Chelsea Finn, and Tengyu Ma. On the expressivity of neural networks for deep reinforcement learning. In *International Conference on Machine Learning*, pages 2627–2637. PMLR, 2020.
- [12] David K Duvenaud, Dougal Maclaurin, Jorge Iparraguirre, Rafael Bombarell, Timothy Hirzel, Alán Aspuru-Guzik, and Ryan P Adams. Convolutional networks on graphs for learning molecular fingerprints. *Advances in neural information processing systems*, 28, 2015.
- [13] David Easley and Jon Kleinberg. *Networks, crowds, and markets: Reasoning about a highly connected world*. Cambridge university press, 2010.
- [14] Jakob Foerster, Ioannis Alexandros Assael, Nando De Freitas, and Shimon Whiteson. Learning to communicate with deep multi-agent reinforcement learning. *Advances in neural information processing systems*, 29, 2016.
- [15] Jakob Foerster, Gregory Farquhar, Triantafyllos Afouras, Nantas Nardelli, and Shimon Whiteson. Counterfactual multi-agent policy gradients. In *Proceedings of the AAAI conference on artificial intelligence*, volume 32, 2018.
- [16] Vikas Garg, Stefanie Jegelka, and Tommi Jaakkola. Generalization and representational limits of graph neural networks. In *International Conference on Machine Learning*, pages 3419–3430. PMLR, 2020.
- [17] Justin Gilmer, Samuel S Schoenholz, Patrick F Riley, Oriol Vinyals, and George E Dahl. Neural message passing for quantum chemistry. In *International conference on machine learning*, pages 1263–1272. PMLR, 2017.

- [18] Jayesh K Gupta, Maxim Egorov, and Mykel Kochenderfer. Cooperative multi-agent control using deep reinforcement learning. In *International conference on autonomous agents and multiagent systems*, pages 66–83. Springer, 2017.
- [19] Will Hamilton, Zhitao Ying, and Jure Leskovec. Inductive representation learning on large graphs. *Advances in neural information processing systems*, 30, 2017.
- [20] Todd Hester, Matej Vecerik, Olivier Pietquin, Marc Lanctot, Tom Schaul, Bilal Piot, Dan Horgan, John Quan, Andrew Sendonaris, Ian Osband, et al. Deep q-learning from demonstrations. In *Proceedings of the AAAI Conference on Artificial Intelligence*, volume 32, 2018.
- [21] Guangzheng Hu, Yuanheng Zhu, Dongbin Zhao, Mengchen Zhao, and Jianye Hao. Event-triggered multi-agent reinforcement learning with communication under limited-bandwidth constraint. *arXiv preprint arXiv:2010.04978*, 2020.
- [22] Hengyuan Hu and Jakob N Foerster. Simplified action decoder for deep multi-agent reinforcement learning. *8th International Conference on Learning Representations (ICLR)*, 2020.
- [23] Jiechuan Jiang and Zongqing Lu. Learning attentional communication for multi-agent cooperation. *Advances in neural information processing systems*, 31, 2018.
- [24] Jiechuan Jiang, Chen Dun, Tiejun Huang, and Zongqing Lu. Graph convolutional reinforcement learning. *International Conference on Learning Representations*, 2020.
- [25] Daewoo Kim, Sangwoo Moon, David Hostallero, Wan Ju Kang, Taeyoung Lee, Kyunghwan Son, and Yung Yi. Learning to schedule communication in multi-agent reinforcement learning. *International Conference on Learning Representations*, 2019.
- [26] Risi Kondor, Hy Truong Son, Horace Pan, Brandon Anderson, and Shubhendu Trivedi. Covariant compositional networks for learning graphs. *arXiv preprint arXiv:1801.02144*, 2018.
- [27] Sheng Li, Jayesh K Gupta, Peter Morales, Ross Allen, and Mykel J Kochenderfer. Deep implicit coordination graphs for multi-agent reinforcement learning. *International Conference on Autonomous Agents and Multiagent Systems (AAMAS)*, 2021.
- [28] Michael L Littman. Markov games as a framework for multi-agent reinforcement learning. In *Machine learning proceedings 1994*, pages 157–163. Elsevier, 1994.
- [29] Yong Liu, Weixun Wang, Yujing Hu, Jianye Hao, Xingguo Chen, and Yang Gao. Multi-agent game abstraction via graph attention neural network. In *Proceedings of the AAAI Conference on Artificial Intelligence*, volume 34, pages 7211–7218, 2020.
- [30] Andreas Loukas. What graph neural networks cannot learn: depth vs width. *International Conference on Learning Representations (ICLR)*, 2020.
- [31] Andreas Loukas. How hard is to distinguish graphs with graph neural networks? *Advances in neural information processing systems*, 33:3465–3476, 2020.
- [32] Ryan Lowe, Yi I Wu, Aviv Tamar, Jean Harb, OpenAI Pieter Abbeel, and Igor Mordatch. Multi-agent actor-critic for mixed cooperative-competitive environments. *Advances in neural information processing systems*, 30, 2017.
- [33] Aleksandra Malysheva, Tegg Taekyong Sung, Chae-Bong Sohn, Daniel Kudenko, and Aleksei Shpilman. Deep multi-agent reinforcement learning with relevance graphs. *arXiv preprint arXiv:1811.12557*, 2018.
- [34] Christopher Morris, Martin Ritzert, Matthias Fey, William L Hamilton, Jan Eric Lenssen, Gaurav Rattan, and Martin Grohe. Weisfeiler and leman go neural: Higher-order graph neural networks. In *Proceedings of the AAAI conference on artificial intelligence*, volume 33, pages 4602–4609, 2019.
- [35] Christopher Morris, Yaron Lipman, Haggai Maron, Bastian Rieck, Nils M Kriege, Martin Grohe, Matthias Fey, and Karsten Borgwardt. Weisfeiler and leman go machine learning: The story so far. *arXiv preprint arXiv:2112.09992*, 2021.

[36] Ryan L Murphy, Balasubramaniam Srinivasan, Vinayak Rao, and Bruno Ribeiro. Janossy pooling: Learning deep permutation-invariant functions for variable-size inputs. *International Conference on Learning Representations (ICLR)*, 2019.

[37] Yaru Niu, Rohan Paleja, and Matthew Gombolay. Multi-agent graph-attention communication and teaming. In *Proceedings of the 20th International Conference on Autonomous Agents and MultiAgent Systems*, pages 964–973, 2021.

[38] Hoang Nt and Takanori Maehara. Revisiting graph neural networks: All we have is low-pass filters. *arXiv preprint arXiv:1905.09550*, 2019.

[39] Frans A Oliehoek. Decentralized pomdps. In *Reinforcement Learning*, pages 471–503. Springer, 2012.

[40] Kenta Oono and Taiji Suzuki. Graph neural networks exponentially lose expressive power for node classification. *ICLR*, 2020.

[41] Georgios Papoudakis, Filippos Christianos, Lukas Schäfer, and Stefano V Albrecht. Benchmarking multi-agent deep reinforcement learning algorithms in cooperative tasks. *Advances in Neural Information Processing Systems Track on Datasets and Benchmarks*, 2021.

[42] Pál András Papp, Karolis Martinkus, Lukas Faber, and Roger Wattenhofer. Dropgnn: random dropouts increase the expressiveness of graph neural networks. *Advances in Neural Information Processing Systems*, 34, 2021.

[43] Peng Peng, Ying Wen, Yaodong Yang, Quan Yuan, Zhenkun Tang, Haitao Long, and Jun Wang. Multiagent bidirectionally-coordinated nets: Emergence of human-level coordination in learning to play starcraft combat games. *arXiv preprint arXiv:1703.10069*, 2017.

[44] Chao Qu, Hui Li, Chang Liu, Junwu Xiong, James Zhang, Wei Chu, Weiqiang Wang, Yuan Qi, and Le Song. Intention propagation for multi-agent reinforcement learning. *arXiv preprint arXiv:2004.08883*, 2020.

[45] Tabish Rashid, Mikayel Samvelyan, Christian Schroeder, Gregory Farquhar, Jakob Foerster, and Shimon Whiteson. Qmix: Monotonic value function factorisation for deep multi-agent reinforcement learning. In *International Conference on Machine Learning*, pages 4295–4304. PMLR, 2018.

[46] Ifrah Saeed, Andrew C Cullen, Sarah Erfani, and Tansu Alpcan. Domain-aware multiagent reinforcement learning in navigation. In *2021 International Joint Conference on Neural Networks (IJCNN)*, pages 1–8. IEEE, 2021.

[47] Ryoma Sato, Makoto Yamada, and Hisashi Kashima. Random features strengthen graph neural networks. In *Proceedings of the 2021 SIAM International Conference on Data Mining (SDM)*, pages 333–341. SIAM, 2021.

[48] Martin Simonovsky and Nikos Komodakis. Dynamic edge-conditioned filters in convolutional neural networks on graphs. In *Proceedings of the IEEE conference on computer vision and pattern recognition*, pages 3693–3702, 2017.

[49] Amanpreet Singh, Tushar Jain, and Sainbayar Sukhbaatar. Learning when to communicate at scale in multiagent cooperative and competitive tasks. *ICLR*, 2019.

[50] Kaushik Subramanian, Charles L Isbell Jr, and Andrea L Thomaz. Exploration from demonstration for interactive reinforcement learning. In *Proceedings of the 2016 international conference on autonomous agents & multiagent systems*, pages 447–456, 2016.

[51] Sainbayar Sukhbaatar, Rob Fergus, et al. Learning multiagent communication with backpropagation. *Advances in neural information processing systems*, 29:2244–2252, 2016.

[52] Chuxiong Sun, Bo Wu, Rui Wang, Xiaohui Hu, Xiaoya Yang, and Cong Cong. Intrinsic motivated multi-agent communication. In *Proceedings of the 20th International Conference on Autonomous Agents and MultiAgent Systems*, pages 1668–1670, 2021.

[53] Ardi Tampuu, Tambet Matiisen, Dorian Kodelja, Ilya Kuzovkin, Kristjan Korjus, Juhan Aru, Jaan Aru, and Raul Vicente. Multiagent cooperation and competition with deep reinforcement learning. *PloS one*, 12(4):e0172395, 2017.

[54] Justin K Terry, Nathaniel Grammel, Ananth Hari, Luis Santos, and Benjamin Black. Revisiting parameter sharing in multi-agent deep reinforcement learning. *arXiv preprint arXiv:2005.13625*, 2020.

[55] Michel Tokic. Adaptive ε -greedy exploration in reinforcement learning based on value differences. In *Annual Conference on Artificial Intelligence*, pages 203–210. Springer, 2010.

[56] Petar Veličković, Guillem Cucurull, Arantxa Casanova, Adriana Romero, Pietro Lio, and Yoshua Bengio. Graph attention networks. *International Conference on Learning Representations (ICLR)*, 2018.

[57] Clement Vignac, Andreas Loukas, and Pascal Frossard. Building powerful and equivariant graph neural networks with structural message-passing. *Advances in Neural Information Processing Systems*, 33:14143–14155, 2020.

[58] Ziyu Wang, Victor Bapst, Nicolas Heess, Volodymyr Mnih, Remi Munos, Koray Kavukcuoglu, and Nando de Freitas. Sample efficient actor-critic with experience replay. *International Conference on Learning Representations (ICLR)*, 2017.

[59] Pascal Weber, Daniel Wälchli, Mustafa Zeqiri, and Petros Koumoutsakos. Remember and forget experience replay for multi-agent reinforcement learning. *arXiv preprint arXiv:2203.13319*, 2022.

[60] Boris Weisfeiler and Andrei Leman. The reduction of a graph to canonical form and the algebra which appears therein. *NTI, Series*, 2(9):12–16, 1968.

[61] Keyulu Xu, Weihua Hu, Jure Leskovec, and Stefanie Jegelka. How powerful are graph neural networks? *International Conference on Learning Representations (ICLR)*, 2019.

[62] Yaodong Yang, Rui Luo, Minne Li, Ming Zhou, Weinan Zhang, and Jun Wang. Mean field multi-agent reinforcement learning. In *International Conference on Machine Learning*, pages 5571–5580. PMLR, 2018.

[63] Chao Yu, Akash Velu, Eugene Vinitsky, Yu Wang, Alexandre Bayen, and Yi Wu. The surprising effectiveness of mappo in cooperative, multi-agent games. *arXiv preprint arXiv:2103.01955*, 2021.

[64] Sai Qian Zhang, Qi Zhang, and Jieyu Lin. Efficient communication in multi-agent reinforcement learning via variance based control. *Advances in Neural Information Processing Systems*, 32, 2019.

[65] Sai Qian Zhang, Qi Zhang, and Jieyu Lin. Succinct and robust multi-agent communication with temporal message control. *Advances in Neural Information Processing Systems*, 33: 17271–17282, 2020.

[66] Jian Zhao, Mingyu Yang, Xunhan Hu, Wengang Zhou, and Houqiang Li. Dqmix: A distributional perspective on multi-agent reinforcement learning. *arXiv preprint arXiv:2202.10134*, 2022.

[67] Changxi Zhu, Mehdi Dastani, and Shihan Wang. A survey of multi-agent reinforcement learning with communication. *arXiv preprint arXiv:2203.08975*, 2022.

Checklist

1. For all authors...
 - (a) Do the main claims made in the abstract and introduction accurately reflect the paper’s contributions and scope? **[Yes]**

- (b) Did you describe the limitations of your work? **[Yes]** The theoretical assumptions are stated concretely in Section 3. The limitation of our empirical analysis not providing a complete picture relating expressivity to performance on MARL environments is clearly stated in the abstract and introduction.
- (c) Did you discuss any potential negative societal impacts of your work? **[N/A]** We identified no negative societal impacts.
- (d) Have you read the ethics review guidelines and ensured that your paper conforms to them? **[Yes]**

2. If you are including theoretical results...

- (a) Did you state the full set of assumptions of all theoretical results? **[Yes]** Assumptions are stated in Section 3 and Appendix B.
- (b) Did you include complete proofs of all theoretical results? **[Yes]** Full proofs for all of our theoretical results are provided in Appendix B.

3. If you ran experiments...

- (a) Did you include the code, data, and instructions needed to reproduce the main experimental results (either in the supplemental material or as a URL)? **[Yes]** Code, environments, and instructions for reproducibility are included in the supplemental material.
- (b) Did you specify all the training details (e.g., data splits, hyperparameters, how they were chosen)? **[Yes]** All training details are stated in Section 4.1 and Appendix C.
- (c) Did you report error bars (e.g., with respect to the random seed after running experiments multiple times)? **[Yes]** 95% CI error bars are reported for all results in Section 4.2 and Appendix C.
- (d) Did you include the total amount of compute and the type of resources used (e.g., type of GPUs, internal cluster, or cloud provider)? **[Yes]** The above details are provided in Appendix D.

4. If you are using existing assets (e.g., code, data, models) or curating/releasing new assets...

- (a) If your work uses existing assets, did you cite the creators? **[Yes]** [24, 37]
- (b) Did you mention the license of the assets? **[Yes]** See Appendix C.1.
- (c) Did you include any new assets either in the supplemental material or as a URL? **[Yes]** New environments and code provided in the supplemental material.
- (d) Did you discuss whether and how consent was obtained from people whose data you’re using/curating? **[N/A]**
- (e) Did you discuss whether the data you are using/curating contains personally identifiable information or offensive content? **[N/A]**

5. If you used crowdsourcing or conducted research with human subjects...

- (a) Did you include the full text of instructions given to participants and screenshots, if applicable? **[N/A]**
- (b) Did you describe any potential participant risks, with links to Institutional Review Board (IRB) approvals, if applicable? **[N/A]**
- (c) Did you include the estimated hourly wage paid to participants and the total amount spent on participant compensation? **[N/A]**

A Full Background

In this appendix, for technical and theoretical completeness, we expand upon information given in the background of the paper.

A.1 Multi-Agent Reinforcement Learning

We consider the case of Decentralized Partially Observable Markov Decision Processes (Dec-POMDPs) [28] augmented with communication between agents. In a Dec-POMDP, at each timestep t every agent $i \in \{1, \dots, N\}$ gets a local observation o_i^t , takes an action a_i^t , and receives a reward r_i^t . The objective is to maximize the agent rewards over the actions. We consider two agent paradigms: value-based and actor-critic.

In value-based methods, such as MADQN [53], the aim is to learn a function Q_θ with parameters θ that estimates the value of taking an action a_i after observing o_i . Such methods are often trained using a replay buffer, to which tuples (O, A, O', R) are added, where $O = \{o_1, \dots, o_N\}$ is the set of observations, A is the set of actions, O' is the set of next observations, and R is the set of rewards. If the environment includes communication, the underlying communication graph C can also be included in the replay buffer. These experiences are added to the buffer whilst the agents interact with the environment. To collect diverse experiences, methods such as ϵ -greedy exploration [55] can be used. For training, random minibatches of size B are sampled from the buffer, and loss similar to the following is minimized:

$$L(\theta) = \frac{1}{B} \sum_{b=1}^B \frac{1}{N} \sum_{i=1}^N (y_i - Q_\theta(o_i, a_i))^2$$

where $y_i = r_i + \gamma \max_{a'} Q_{\theta'}(o_i', a_i')$. In this formula, $Q_{\theta'}$ is referred to as the *target network*, and its parameters θ' are updated softly or intermittently from θ during training.

In actor-critic methods such as MADDPG [32], the aim is to learn a policy function π_θ that maps observations onto distributions over actions, where the action most likely to maximize the reward is assigned the highest probability. The policy gradient is estimated by the following:

$$\nabla_\theta J(\theta) = \mathbb{E}_{o \sim \rho^\pi, a \sim \pi_\theta} \left[\sum_{t=1}^T \nabla_\theta \log \pi_\theta(a_t | o_t) (R_t - V(o_t)) \right]$$

where ρ^π is the observation distribution, π_θ is the policy distribution, $R_t = \sum_{t'=t}^T \gamma^{t'-t} r(s_{t'}, a_{t'})$ is the discounted reward, and V is a learned value function, used to decrease the variance of the estimated policy gradient.

For brevity, we collectively refer to the policy network / value function or Q-network as the *actor network*. Often in MARL, instead of learning an actor network for each agent, a single shared network will be used for all agents. For example, COMA [15], Q-Mix [45], and Mean Field RL [62] all share parameters in their neural networks. This parameter sharing typically yields faster and more stable training [18].

A.2 Communication in MARL

Many environments require agents to coordinate to solve tasks. Communication is crucial for enabling this. Foerster et al. [14], Sukhbaatar et al. [51] were among the first to propose learned communication in multi-agent reinforcement learning. Since then, many different methods for communication in MARL have been proposed [67]. When communicating, there is a helpful structural inductive bias which can be used: the order in which incoming messages from other agents are processed should not affect the outcome. More formally: agents ought to be *permutation invariant* when using incoming messages. A function ρ is permutation invariant if for any input $X = (x_1, x_2, \dots, x_k)$ and any permutation σ on X , $\rho(X) = \rho(\sigma \circ X)$.

In Section 3.1, we define Graph Decision Networks (GDNs) using the framework of GNNs, a neural architecture which respects permutation invariance between nodes when doing message passing.

Many of the most successful models for MARL communication fall within this paradigm, including CommNet [51], IC3Net [49], GA-Comm [29], MAGIC [37], Agent-Entity Graph [2], IP [44], TARMAC [9], IMMAC [52], DGN [24], VBC [64], MAGNet [33], and TMC [65]. Other models such as ATOC [23] and BiCNet [43] do not fall within the paradigm since they use LSTMs for combining messages, which are not permutation invariant, and models such as RIAL, DIAL [14], ETCNet [21], and SchedNet [25] do not since they used a fixed message-passing structure.

A.3 Graph Neural Networks

A graph consists of nodes and edges connecting them. Nodes and edges can have attributes (also referred to as features or labels), which often take the form of real vectors. Formally, we define an attributed graph G as a triple (V, E, a) , where $V(G)$ is a finite set of nodes, $E(G) \subseteq \{(u, v) \mid u, v \in V(G)\}$ is a set of directed edges, and $a : V(G) \cup E(G) \rightarrow \mathbb{R}^d$ is an attribute function where $d > 0$. For $w \in V(G) \cup E(G)$, $a(w)$ is the attribute of w . Undirected graphs are ones in which $E(G)$ is a symmetric relation on $V(G)$. Graphs are found in many different areas of application, leading to a plethora of research of how to learn using graph structured data [3, 13, 48].

When considering functions operating on graphs, it is sensible to demand permutation invariance and equivariance. Intuitively: the output of any function on a graph should not depend on the order of the nodes (invariance), and if the function provides outputs for each node, then re-ordering the nodes of the input graph should be equivalent to applying the same re-ordering to the output values (equivariance). Formally, let $S(V(G))$ be the set of all permutations of $V(G)$, D a set of graphs, and L a set of potential output attributes (e.g. \mathbb{R}^3). Then a function $f : D \rightarrow L$ is *invariant* if:

$$\forall \text{ graphs } G \in D, \forall \text{ permutations } \sigma \in S(V(G)), f(G) = f(\sigma \circ G)$$

A function $f : D \rightarrow L^{|V(G)|}$ is likewise *equivariant* if instead $f(\sigma \circ G) = \sigma \circ f(G)$.

GNNs belong to a class of neural methods that operate upon graphs. The term is often used to refer to a large variety of models; in this paper, we define the term ‘‘Graph Neural Networks’’ to correspond to the definition of Message Passing Neural Networks (MPNNs) by Gilmer et al. [17], which is the most common GNN architecture. Notable instances of this architecture include Graph Convolutional Networks (GCNs) [12], GraphSAGE [19], and Graph Attention Networks (GATs) [56]. A GNN consists of multiple message-passing layers, where each layer aggregates node attribute information to every node from its neighbours in the graph, and then uses the aggregated information with the current node attribute to assign a new value to the attribute, passing all updated node attributes to the next GNN layer. GNNs are often augmented with global readouts, where in each layer we also aggregate a feature vector for the whole graph and use it in conjunction with the local aggregations [4]. For layer m and node i with current attribute v_i^m , the new attribute v_i^{m+1} is computed as

$$v_i^{m+1} := f_{\text{update}}^{\theta_m}(v_i^m, f_{\text{aggr}}^{\theta'_m}(\{v_j^m \mid j \in N(i)\}), f_{\text{read}}^{\theta''_m}(\{v_j^m \mid j \in V(G)\}))$$

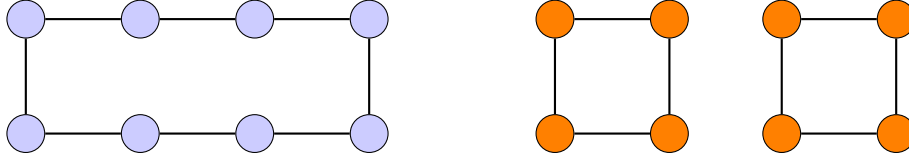
where $N(i)$ is all nodes with edges connecting to i and $\theta_m, \theta'_m, \theta''_m$ are the (possibly trainable) parameters of the update, aggregation, and readout functions for layer m . Parameters may be shared between layers, e.g. $\theta_0 = \theta_1$. The functions $f_{\text{aggr}}^{\theta'_m}, f_{\text{read}}^{\theta''_m}$ are permutation invariant. A global graph feature can be computed by having a final *readout layer* which aggregates all node attributes into a single feature. Importantly, GNNs are invariant / equivariant graph functions.

A.4 Expressivity and Related Work

Morris et al. [34], Xu et al. [61] concurrently showed that any GNN cannot be more powerful than the 1-WL graph-coloring algorithm in terms of distinguishing non-isomorphic graphs, meaning that there are pairs of non-isomorphic graphs G_1, G_2 which for any GNN f , $f(G_1) = f(G_2)$. Morris et al. [34] also define k -GNNs, a class of higher-order GNNs which have the same expressive power as the k -WL algorithm. Chen et al. [8] prove that GNNs cannot count certain types of sub-structures and that certain higher-order GNNs can.

Garg et al. [16] prove that some important graph properties cannot be computed by GNNs, and also provide data dependent generalization bounds for GNNs. Nt and Maehara [38] show that GNNs

Figure 2: A pair of graphs indistinguishable by 1-WL



only perform low-pass filtering on attributes and investigate their resilience to noise in the features. Barceló et al. [4] prove a direct correspondence between GNNs and Boolean classifiers expressed in the first-order logic fragment FOC_2 .

Loukas [30] demonstrates how GNNs lose expressivity when their depth and width are restricted. Loukas [31] further analyzes the expressive power of GNNs with respect to their *communication capacity*, a measure of how much information the nodes of a network can exchange during message-passing. Oono and Suzuki [40] analyze the expressive power of GNNs as the number of layers tends to infinity, proving that under certain conditions, the output will carry no information other than node degrees and connected components.

In the space of expressivity for reinforcement learning, Dong et al. [11] compare model-free reinforcement learning with the model-based approaches with respect to the expressive power of neural networks for policies and Q-functions. Castellini et al. [6] empirically evaluate the representational power of different value-based RL network architectures using a series of one-shot games. The simplistic games capture many of the issues that arise in the multi-agent setting, such as the lack of an explicit coordination mechanism, which provides good motivation for the inclusion of communication.

A.5 Weisfeiler-Lehman Expressivity

1-WL [60] is a graph coloring algorithm that tests if two graphs are non-isomorphic by iteratively re-coloring the nodes. Given an initial graph coloring corresponding to the node labels, in each iteration, two nodes with the same color get assigned different colors if the number of identically colored neighbors is not equal. If, at some point, the number of nodes assigned a specific color is different across the two graphs, the algorithm asserts that the graphs are not isomorphic. However, there are non-isomorphic graphs which the algorithm will not recognize as non-isomorphic, e.g. in Figure 2. Morris et al. [34], Xu et al. [61] proved that for any two non-isomorphic graphs indistinguishable by 1-WL, there is no GNN that can produce different outputs for the two graphs. Furthermore, there is a fundamental link between this graph separation power and function approximation power. Chen et al. [7] proved that a class of models can separate all graphs if and only if it can approximate any continuous invariant function.

There are several GNN architectures which are designed to go beyond 1-WL expressivity. Morris et al. [34] propose k -GNNs, which are equivalent to the k -WL algorithm. Morris et al. [35] also show the link between k -order equivariant graph networks (EGNs) [26] and the k -WL algorithm. Other attempts also include using unique node IDs and passing matrix features [57], relational pooling [36], and random dropouts [42]. Morris et al. [35] provide an overview of many such higher-order models. However, many of these models do not scale well and are computationally infeasible in practice.

A.6 Random Node Initialization

Sato et al. [47] propose augmenting GNNs with *random node initialization* (RNI), where for each node in the input graph, a number of randomly sampled values are concatenated to the original node attribute. For all graphs / nodes, the random values are sampled from the same distribution. Abboud et al. [1] prove that such GNNs are universal and can approximate any permutation invariant graph function. Technically, random initialization breaks the node invariance in GNNs, since the result of the message passing will depend on the structure of the graph as well as the values of the random initializations. However, when one views the model as computing a random variable, the random variable is still invariant when using RNI. In expectation, the mean of random features will be used for GNN predictions, and is the same across each node. However, the variability of the random

samples allow the GNN to discriminate between nodes that have different random initializations, breaking the 1-WL upper bound.

The above is formally described by Abboud et al. [1] as follows. Let G_n be the class of all n -node graphs (i.e. graphs that consist of at most n nodes) and let $f : G_n \rightarrow \mathbb{R}$. We say that a randomized function X that associates with every graph $G \in G_n$ a random variable $X(G)$ is an (ϵ, δ) -approximation of f if for all $G \in G_n$ it holds that $\Pr(|f(G) - X(G)| \leq \epsilon) \geq 1 - \delta$. Note that an MPNN N with RNI computes such functions X . If X is computed by N , we say that N (ϵ, δ) -approximates f .

They state the following theorem:

Theorem. *Let $n \geq 1$ and let $f : G_n \rightarrow \mathbb{R}$ be invariant. Then for all $\epsilon, \delta > 0$, there is an MPNN with RNI that (ϵ, δ) -approximates f .*

A.7 Other Conditions for Expressivity

For another method of analyzing GDN expressivity through the lens of GNNs, consider the work of Loukas [31], which defines the *communication capacity / complexity* c_g of GNNs, a measure of how much information the nodes can exchange during message passing. The following intuitive theorem is proven:

Theorem. *Let f be an MPNN with d layers, where each has width w_m (attribute size), message size a_m (output of aggregation), and a global state of size γ_m (output of global readout). For any disjoint partition of V into V_a, V_b , where $\text{cut}(V_a, V_b)$ is the size of the smallest cut separating V_a, V_b :*

$$c_g \leq \text{cut}(V_a, V_b) \sum_{m=1}^d \min(a_m, w_m) + \sum_{m=1}^d \gamma_m$$

Loukas [31] prove that MPNNs with sub-quadratic and sub-linear capacity (with respect to the number of nodes) cannot compute the isomorphism class of graphs and trees respectively, demonstrating that capacity is an important consideration for GNN expressivity. This is also supported empirically. When designing a GNN model, we have no control over the structure of the input graphs. Thus, all features apart from $\text{cut}(V_a, V_b)$ are important considerations for the architecture. In GDNs, this corresponds to the message sizes m and the number of rounds of message passing d . We provide the practical recommendation that when choosing $\{m, d\}$, one ought to scale them such that $m \cdot d \in \Omega(n^2)$, where n is the number of agents. In environments where communication is limited by range or obstacles, the number of rounds of message passing is also important when it comes to increasing an agent's *receptive field*: from how many edges away information is propagated to the agent.

B Proofs

Before we dive into the proofs, here follows a few brief notes / clarifications on the theory outlined in the paper.

Neural Network Function Approximation GNNs consist of the composition of update, aggregate, and readout functions, all of which are approximated by neural networks. Thus, given that neural networks are only universal approximators for *continuous* functions, if standard neural architectures are used within GNNs, then GNNs can only ever approximate continuous functions. As such, if standard neural networks are used, then all universal approximation results in this paper require the additional assumption that the function being approximated is continuous.

GNN Vector Targeting For all theorems and proofs that utilize \mathbb{R} , such as equivariant graph functions with codomain \mathbb{R}^n , note that the scalar \mathbb{R} can be replaced with the vector \mathbb{R}^k for any $k > 1$, whilst maintaining correctness.

To demonstrate this, let $k > 1$ and consider an equivariant graph function $f : G_n \rightarrow (\mathbb{R}^k)^n$ that we are trying to approximate. We can instead approximate k different functions f_1, f_2, \dots, f_k with $f_j : G_n \rightarrow \mathbb{R}^n$, such that $\forall G \in G_n \forall i \in \{1, 2, \dots, n\}, f(G)_i = (f_1(G)_i, f_2(G)_i, \dots, f_n(G)_i)$. These functions can be approximated using the theoretical results we currently have, with GNNs g_1, g_2, \dots, g_k . We will simulate the application of all of these GNNs using a single GNN.

Thus, f can also be approximated by the following construction: use an initial GNN layer with the update function defined such that $f_{\text{update}}(v) := (v, v, \dots, v)$, where v is transformed into k copies of itself. Then, define the update, aggregation, and readout functions of each layer using the GNNs g_1, g_2, \dots, g_k , conditioning each one on a portion of the node attributes. For example, the update function of layer m for node i on attribute (v_1, v_2, \dots, v_k) is defined by $f_{\text{update}}^{\theta_m}(v_1, v_2, \dots, v_k) := (g_1^{\theta_m}(\text{update}(v_1)), \dots, g_k^{\theta_m}(\text{update}(v_k)))$.

This construction simulates the application of f_1, f_2, \dots, f_k in parallel and thus approximates f .

Recurrent GNNs In Section 3.1, it is stated that models with recurrent networks also fall within the GDN paradigm, where the hidden or cell states for the networks can be considered as part of the agent observations. In this section, we briefly demonstrate how this can be done.

More concretely, consider a scenario with n agents, where each GNN layer $m \in R \subseteq \{1, 2, \dots, M\}$ uses hidden or cell states $C^{m-1} := \{c_1^{m-1}, c_2^{m-1}, \dots, c_n^{m-1}\}$. In this case, R represents the list of layers that use recurrent networks. In a non-recurrent GNN, if layer m is expressed as a function, it takes as input only the node attributes from the previous layer: V^{m-1} . In the recurrent case, it also takes C^{m-1} as input: $m(V^{m-1}, C^{m-1})$.

To express this in terms of a non-recurrent GNN, instead modify the initial node attributes $V^0 = \{v_1^0, v_2^0, \dots, v_n^0\}$ such that for each node i , $v_i^0 := (v_i^0, c_i^1, c_i^2, \dots, c_i^{m'})$, where $m' := \max \text{ value in } R$. Then in each layer $m \in \{1, 2, \dots, M\}$ of the GNN and for each node i , only update v_i^{m-1} to v_i^m in $(v_i^{m-1}, c_i^1, c_i^2, \dots, c_i^{m'})$, leaving all other portions of the attribute as-is. As input to the update, if $m \in R$ then use only v_i^{m-1} and c_i^m , and otherwise use only v_i^{m-1} .

The above-described non-recurrent GNN computes the exact same output as the recurrent GNN it is emulating, by simply pulling hidden or cell states from a portion of the initial node attributes that has been set aside for them.

B.1 Theorem 1

Theorem. *Given a GDN f , observations $O = \{o_1, \dots, o_n\}$, and communication graph G such that nodes i and j are similar in G and $o_i = o_j$, then it holds that $f(O)_i = f(O)_j$.*

Proof. Since f is a GDN, there exists a GNN g whose output when operating on the graph G' , equal to G augmented with initial node attributes of O , coincides with that of f on O .

Since i and j are similar in G and $o_i = o_j$, i and j are similar in G' (using the same automorphism). Also g is a GNN, so g is an equivariant function on G' . Thus

$$\forall \text{ graphs } G, \forall \text{ permutations } \sigma \in S(V(G)), f(\sigma \circ G) = \sigma \circ f(G)$$

Define $\sigma := (i \ j)$, the permutation that maps $i \rightarrow j$ and $j \rightarrow i$, while mapping all other nodes to themselves. Note that since i and j are similar, $\sigma \circ G' = G'$. Furthermore, $\sigma = \sigma^{-1}$. So

$$f(O)_i = g(G')_i = (\sigma^{-1} \circ \sigma \circ g(G'))_i = (\sigma^{-1} \circ g(\sigma \circ G'))_i = g(\sigma \circ G')_j = g(G')_j = f(O)_j$$

□

B.2 Theorem 2

Theorem. *Let $n \geq 1$ and let $f : G_n \rightarrow \mathbb{R}^n$ be equivariant. Then for all $\epsilon, \delta > 0$, there is a GNN with RNI that (ϵ, δ) -approximates f .*

Proof. For this proof, we assume the reader to be familiar with the proofs in the appendix of Abboud et al. [1], as we make use of their definitions, notation, lemmas, and proofs.

Abboud et al. [1] state and prove the following. Let G_n be the class of all n -node graphs (i.e., graphs that consist of at most n nodes) and let $f : G_n \rightarrow \mathbb{R}$. We say that a randomized function X that associates with every graph $G \in G_n$ a random variable $X(G)$ is an (ϵ, δ) -approximation of f if for all $G \in G_n$ it holds that $\Pr(|f(G) - X(G)| \leq \epsilon) \geq 1 - \delta$. Note that an MPNN N with RNI computes such functions X . If X is computed by N , we say that N (ϵ, δ) -approximates f .

Theorem. *Let $n \geq 1$ and let $f : G_n \rightarrow \mathbb{R}$ be invariant. Then for all $\epsilon, \delta > 0$, there is an MPNN with RNI that (ϵ, δ) -approximates f .*

We extend this theorem to equivariant functions. Recall that we define the following. Let G_n be the class of all n -node graphs. Let $f : G_n \rightarrow \mathbb{R}^n$, a graph function which outputs a real value for each node in $V(G)$. We say that a randomized function X that associates with every graph $G \in G_n$ a sequence of random variables $X_1(G), X_2(G), \dots, X_n(G)$, one for each node, is an (ϵ, δ) -approximation of f if for all $G \in G_n$ it holds that $\forall i \in \{1, 2, \dots, n\}, \Pr(|f(G)_i - X_i(G)| \leq \epsilon) \geq 1 - \delta$, where $f(G)_i$ is the output of $f(G)$ for node i . Note that a GNN h with RNI computes such functions X . If X is computed by h , we say h (ϵ, δ) -approximates f .

We adapt the proof of Abboud et al. [1], shown in their appendix, to correspond to equivariant functions instead. Notice that equivariant functions have their output at the node level instead of the graph level, so instead of identifying graphs with C^2 -sentences that have no input variables, we identify a graph and a node in the graph by a 1-variable formula $\phi(v)$, where v identifies the node.

Lemma A.3 from Abboud et al. [1] proves that for every individualized colored graph G there is a C^2 -sentence χ_G that identifies G . Thus, for every individualized colored graph G and node u , the formula $\phi_{G,u}(v) := \chi_G \wedge \text{Node}_u(v)$ identifies G and the node u , where $\text{Node}_u(v)$ is a Boolean function that is only true when $u = v$. In fact, $\phi_{G,u}(v) := \phi_u(v) := \text{Node}_u(v)$ already identifies G by identifying the exact node.

We can similarly adapt Lemma A.4 and state the following:

Lemma. *Let $h : \mathcal{G}_{n,k} \rightarrow \{0, 1\}^n$ be an equivariant Boolean function. Then there exists a 1-variable formula $\phi_h(v)$ such that for all $G \in \mathcal{G}_{n,k}$ and all $v \in G$ it holds that $[[\phi_h(v)]](G) = h(G)_v$.*

To prove this, let $\mathcal{V} \subseteq \{V(G) \mid G \in \mathcal{G}_{n,k}\}$ be the subset consisting of all nodes u with $h(G)_u = 1$, where G is the graph such that $u \in V(G)$. Then let

$$\phi_h(v) := \bigvee_{u \in \mathcal{V}} \phi_u(v)$$

We eliminate duplicates in the disjunction. Since, up to isomorphism, the class $\mathcal{G}_{n,k}$ is finite, and the number of nodes in each graph is upper-bounded by n , the disjunction over \mathcal{V} is finite and hence $\phi_h(v)$ is well-defined.

We adapt Corollary A.1 in the same way as Lemma A.4. Lemma A.5 can be used as-is to show that RNI yields individualized colored graphs with high probability. From here, the remainder of the proof works analogously, substituting in equivariant functions for invariant ones and $\phi_h(v)$ for ψ_h .

□

B.3 Theorem 3

Theorem. *Let $n \geq 1$ and consider a set T , where each $(G, A) \in T$ is a graph-labels pair, such that $G \in \mathcal{G}_n$ and there is a set of target labels $A_k \in A$ for each orbit $r_k \in R(G)$, with $|A_k| = |r_k|$. Then for all $\epsilon, \delta > 0$ there is a GNN with RNI g which satisfies:*

$$\forall (G, A) \in T \quad \forall r_k \in R(G), \{g(G)_i \mid i \in r_k\} \cong_{\epsilon, \delta} A_k$$

Proof. Recall that we say two sets A, B containing random variables are (ϵ, δ) -equal, denoted $A \cong_{\epsilon, \delta} B$, if there exists a bijection $\tau : A \rightarrow B$ such that $\forall a \in A, \Pr(|a - \tau(a)| \leq \epsilon) \geq 1 - \delta$.

We will define a GNN with RNI g by construction which satisfies the property required in the theorem. We do this in 3 intuitive steps:

1. Define a GNN with RNI f that, for each node, outputs a unique identifier for the orbit of the node and the original RNI value given to the node. Such a GNN exists because the function it is approximating is equivariant.
2. Append n identical layers onto f , each of which identifies the node containing the highest RNI value, gives that node a value from the target set of labels corresponding to its orbit, marks off that particular value as claimed, and sets its RNI value to be small.
3. Append a final layer which extracts only the target labels from the node attributes; these were given to the nodes by the preceding n layers.

First, notice that there exists a GNN with RNI $f : G_n \rightarrow (\mathbb{R}^4)^n$ that approximates the outputs $(n_i, r_i, 0, 0)$ for each node i in the input graph G , where n_i is the random noise initially added by RNI (before any message passing) and r_i is a unique value corresponding to the graph orbit of i . Formally: $r_i = r_j \iff i$ and j are in the same orbit of the same graph (up to isomorphism). Put another way: $r_i = r_j \iff$ there exists an isomorphism $\alpha : G_i \rightarrow G_j$ (the graphs containing nodes i and j , respectively) such that $\alpha(i) = j$.

Such a GNN f exists because the function it is approximating is equivariant, allowing us to use Theorem 2. Without loss of generality, we assume that RNI values are sampled from the interval $(0, 1)$ and that we only augment each node with one RNI value.

We define a GNN with RNI g using f as a starting point: we will append further message-passing layers to f . Append n identical message-passing layers to f , each of which is defined as follows. Each node attribute in these layers will be a tuple (n_i, r_i, c_i, t_i) , where c_i is used as a counter and t_i is used to store the eventual node output value, corresponding to some target label. For this proof, we assume that target labels A_k come from \mathbb{R} , but note that the proof is easily extended to vectors from \mathbb{R} instead. Furthermore, we allow for A_k to be a multiset (i.e. with repeated elements). Define f_{read} by

$$f_{\text{read}}(\{(n_j, r_j, c_j, t_j) \mid j \in V(G)\}) := \text{argmax}_{(n_j, r_j, c_j, t_j) \in \{(n_j, r_j, c_j, t_j) \mid j \in V(G)\}} n_j$$

In other words, f_{read} extracts the tuple containing the maximum value of n_j in the graph. Such a unique maximum exists with probability 1, since finitely many RNI values are sampled from an infinite distribution. Do not define f_{aggr} .

Define f_{update} on the output (n_j, r_j, c_j, t_j) of f_{read} and the current node value (n_i, r_i, c_i, t_i) .

$$f_{\text{update}}((n_i, r_i, c_i, t_i), (n_j, r_j, c_j, t_j)) := \begin{cases} (n_i, r_i, c_i, t_i) & \text{if } r_i \neq r_j \\ (n_i, r_i, c_i + 1, t_i) & \text{if } r_i = r_j \text{ and } n_i \neq n_j \\ (0, r_i, c_i + 1, (A_k)_{c_i}) & \text{if } r_i = r_j \text{ and } n_i = n_j \end{cases}$$

In the above, $(A_k)_{c_i}$ denotes treating the set of target labels A_k as a sequence and retrieving the element with index c_i (first index is 0). The above has access to A_k since it can uniquely identify the input graph and orbit of the node using r_i , by how r_i is defined.

As a consequence of its definition, the update function will retrieve one value from the target labels at a time, updating exactly one node to store this value. If another node j within the same orbit as i is being updated with this value, then the counter of i is incremented to track that a value from the outputs has been claimed. Since the RNI value n_i is set to 0, it ensures that each node will be given exactly one target label after n rounds of message passing.

After appending the above n message-passing layers, append one final layer with only an update function that extracts only the target labels, defined by

$$f_{\text{update}}((0, r_i, c_i, t_i)) := t_i$$

The above construction of g satisfies the probability (δ) and approximation (ϵ) requirements of the property stated in the theorem, since f is an (ϵ, δ) -approximation, a unique maximum RNI value exists for each graph with probability 1, and all other required operations can be ϵ -approximated by neural networks. The exact bijection used to map between the output and target sets will depend on the RNI values of the nodes, since they determine the order in which target values are assigned to node attributes in the construction. Whilst our provided construction requires at least $n + 1$ message-passing layers, more efficient constructions exist using more complex readout functions than simple maximisation. The final update layer can also be merged with the previous layer. However, we presented the above construction due to its simplicity and how easy it is to understand the mechanism.

□

B.4 Theorem 4

Theorem. Let $n \geq 1$ and let $f : G_n \rightarrow \mathbb{R}^n$ be equivariant. Then for all $\epsilon > 0$, there is a GNN with unique node IDs that ϵ -approximates f .

Proof. For this proof, we assume the reader to be familiar with the theorems and proofs of Dasoulas et al. [10], particularly their Theorem 4. First, we need to prove that GNNs with unique node IDs are equivalent to 1-CLIP, which is k -CLIP with $k = 1$.

CLIP is defined as a 3-step process, the first of which is assigning colours to nodes. In CLIP, the essential part of each colouring chosen is that all nodes with the same attributes will be assigned different colours. By representing colours with unique node IDs (using a one-hot encoding) we ensure that the above property holds, since all nodes will be assigned different colours. Since we are considering 1-CLIP, we set $k = 1$ and only sample one colouring, which is the particular set of unique IDs we assign.

Step 2 of CLIP is just standard GNN message-passing on our created coloured graph. Step 3 of CLIP maximizes over all possible colourings, of which we have only one, so the maximization can be dropped. This yields a standard GNN global readout layer. Thus, GNNs with unique node IDs are equivalent to 1-CLIP. Theorem 4 of Dasoulas et al. [10] states the universality of 1-CLIP for invariant functions, which we provide here as a Lemma:

Lemma. The 1-CLIP algorithm with one local iteration is a random representation whose expectation is a universal representation of the space \mathbf{Graph}_m of graphs with node attributes.

They further state that for any colouring, 1-CLIP returns an ϵ -approximation of the target function and that, given sufficient training, the variance can be reduced to an arbitrary precision. The above only applies to invariant functions because it is a representation of the space \mathbf{Graph}_m , which is defined using invariance by permutation of the labels. Note that when defining \mathbf{Graph}_m in this paper, we use $n_{\max} := n$, instead of just considering some arbitrary large n_{\max} .

To apply this theorem to equivariant functions, we need to consider the space \mathbf{Node}_m , which we define to be the set of all nodes from graphs in \mathbf{Graph}_m . \mathbf{Node}_m is Hausdorff as a trivial consequence of \mathbf{Graph}_m being Hausdorff, using the same quotient space of orbits. If we can separate this space in a continuous and concatenable way, then we can utilize Corollary 1 of Dasoulas et al. [10] to show that it is universal. To do this, consider a GNN f which separates the space \mathbf{Graph}_m , which we know exists due to Theorem 4 of Dasoulas et al. [10]. We define a new GNN g using f as a starting point. Substitute the final global readout layer M of f for a new layer with the same readout function, but have the output of the readout be assigned to every node. Formally, define

$$f_{\text{update}}^{\theta_M}(v_i^M, f_{\text{aggr}}^{\theta'_M}(\{v_j^M \mid j \in N(i)\}), f_{\text{read}}^{\theta''_M}(\{v_j^M \mid j \in V(G)\})) := f_{\text{read}}^{\theta''_M}(\{v_j^M \mid j \in V(G)\}),$$

where $f_{\text{read}}^{\theta''_M}$ is the former global readout layer. Then, change the update functions of each layer of f such that a portion of each node attribute is reserved for the unique ID of the node, and do not use or change this ID in each layer of f . Then, after the final layer M , the attribute v_i^{M+1} of each node i will be

$$v_i^{M+1} = (u_i, r_i) := (u_i, f_{\text{read}}^{\theta''_M}(\{v_j^M \mid j \in V(G)\})),$$

where u_i is the unique ID given to node i . Since f separates \mathbf{Graph}_m , r_i uniquely identifies the graph provided in the input. Furthermore, u_i uniquely identifies each node in the input graph. Thus, $v_i^{M+1} = (u_i, r_i)$ uniquely identifies every node in the space \mathbf{Node}_m , meaning that g yields a separable representation of \mathbf{Node}_m . Furthermore, g is continuous and concatenable by its construction, so we can apply Corollary 1 of Dasoulas et al. [10] to state that g is universal.

□

B.5 Theorem 5

Theorem. Let $n \geq 1$ and consider a set T , where each $(G, A) \in T$ is a graph-labels pair, such that $G \in G_n$ and there is a set of target labels $A_k \in A$ for each orbit $r_k \in R(G)$, with $|A_k| = |r_k|$. Then for all $\epsilon > 0$ there is a GNN with unique node IDs g which satisfies:

$$\forall (G, A) \in T \quad \forall r_k \in R(G), \{g(G)_i \mid i \in r_k\} \cong_{\epsilon} A_k$$

Proof. Recall that two sets A, B without random variables are ϵ -equal, denoted $A \cong_{\epsilon} B$, if there exists a bijection $\tau : A \rightarrow B$ such that $\forall a \in A, |a - \tau(a)| \leq \epsilon$.

The proof for this theorem is by construction, where the construction is nearly identical to the one used in the proof of Theorem 3. A GNN f exists due to Theorem 4 instead of Theorem 2. Unique ID values are used instead of RNI values. One-hot encodings can be maximised over in a similar way, by treating them as binary numbers. A unique maximum unique ID will always exist by definition.

The construction otherwise proceeds analogously, except that it presents an ϵ -approximation of each target set instead of an (ϵ, δ) -approximation, since no randomness is used. \square

Table 8: Architecture of the Baselines

Name	Communication Graph	MARL Paradigm	GNN Usage
CommNet [51]	Complete (or environment-based)	Recurrent A2C	Implicit
IC3Net [49]	Complete + Gating	Recurrent A2C	Implicit
TarMAC [9]	Complete + Learned Soft Edges	Recurrent A2C	Implicit GAT
T-IC3Net [49, 9]	Gating + Learned Soft Edges	Recurrent A2C	Implicit GAT
MAGIC [37]	Learned	Recurrent A2C	Explicit GAT
DGN [24]	Environment-based	Q-network	Explicit GCN

C Experiments

In this appendix, we provide full details about our experiments for reproducibility.

C.1 Baseline Communication Methods

For evaluation, we adopt a diverse selection of MARL communication methods which fall under the GDN paradigm. These are shown in Table 8, along with the respective paradigm (whether the method simply falls within GDNs or whether GNNs are explicitly used for communication), the MARL paradigm, and communication graph structure. We use the code provided by Niu et al. [37], Jiang et al. [24] as starting points. The [code](#) of Jiang et al. [24] uses an MIT license and the [code](#) of Niu et al. [37] does not have one. All of the implementations are extended to be able to support multiple rounds of message-passing and the baselines are augmented with the ability for their communication to be masked by the environment (e.g. based on distance or obstacles in the environment).

Sukhbaatar et al. [51] define CommNet, which has a single, basic, learnable communication channel. They define it in such a way that agents can enter and leave the communication range of other agents. It maps directly onto a GDN approach where mean is used for aggregation. Singh et al. [49] define IC3Net, which operates in a similar manner to CommNet, except the communication graph is complete and communication is controlled by gating, meaning each agent can decide whether or not to broadcast to another agent. Das et al. [9] define TarMAC, where a soft attention mechanism is used to decide how much of a message an agent should process. This implicitly yields a complete communication graph, which a graph attention network (GAT) is able to model. TarMAC is also extended to use IC3Net’s reward and communication structure, which we refer to as *T-IC3Net*.

Jiang et al. [24] define DGN, which operates on graphs that arise deterministically from the environment (e.g. based on agent proximity). The model consists of an encoding layer from the observations, two convolutional layers that use multi-head dot-product attention as the convolutional kernel, and a shared Q-network between all agents. There are skip connections between the convolutional layers. Note that among our chosen methods, DGN is the only value-based one. Niu et al. [37] define MAGIC, which learns to construct a communication graph and then uses GNNs to operate on the graph. The Scheduler learns which agents should communicate with each other and outputs a communication graph. The Message Processor then uses GATs for multiple rounds of communication on the graph.

C.2 Environments

Predator-Prey [49, 9, 29, 27, 37] and Traffic Junction [51, 49, 9, 29, 27, 37] are common MARL communication benchmarks. We perform evaluations on them to test how well our universally expressive GDN models perform when there is not necessarily a benefit to having communication expressivity beyond 1-WL. We also introduce two new environments, Drone Scatter and Box Pushing, to respectively test symmetry-breaking and communication expressivity beyond 1-WL.

Predator-Prey, introduced by Singh et al. [49], consists of predators (agents) with limited vision trying to find stationary prey. They can communicate with each other within a range of 5 and at each time step move one grid cell in any cardinal direction. An episode is deemed a success if all agents have found and are sitting on top of the prey. We utilize the “cooperative” reward setting of the environment, meaning that reward is given at each time step proportional to the number of agents on the prey. The environment is demonstrated in Figure 3.

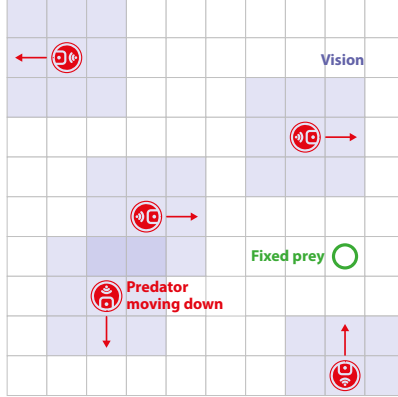


Figure 3: PredatorPrey Environment

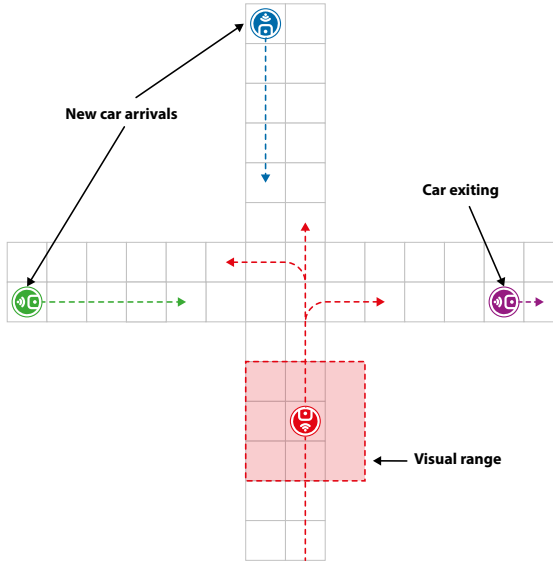


Figure 4: Medium TrafficJunction Environment

Traffic Junction, introduced by Sukhbaatar et al. [51], consists of intersecting roads with cars (agents) driving along them. The agents have limited vision and need to communicate to avoid collisions; an episode is deemed a success if it had no collisions. Each car can communicate with any other car within a range of 3. At each time step, cars enter the environment with a given probability, provided the number of cars in the environment does not exceed the allowed maximum. At each step, a car can either “gas” or “break”, leading to it either moving forward one cell on its route or remaining stationary. We utilize both the “Easy” and “Medium” versions of the environment, which respectively consist of two intersecting 1-way roads and two intersecting 2-way roads. The environment is demonstrated in Figure 4.

The **Drone Scatter** environment is a grid environment, which we design to test the ability of communication models to perform symmetry-breaking. It consists of 4 drones in a 20x20 homogeneous field. The outer lines of the field are marked by fences. The drones can move any of the 4 cardinal directions at each time step. Their goal is to move around and find a target hidden in the field, which they can only notice when they get close to. The drones do not have GPS and can only see directly beneath them using their cameras. They also know which action they took in the last time step. The best way for them to locate the target is to split up and search in different portions of the field. Thus, in the “easy” version of the environment, they are encouraged to do this by being given a reward based on how far away they are from the rest of the drones. They are also always given a reward for finding the target. The environment is demonstrated in Figure 5.

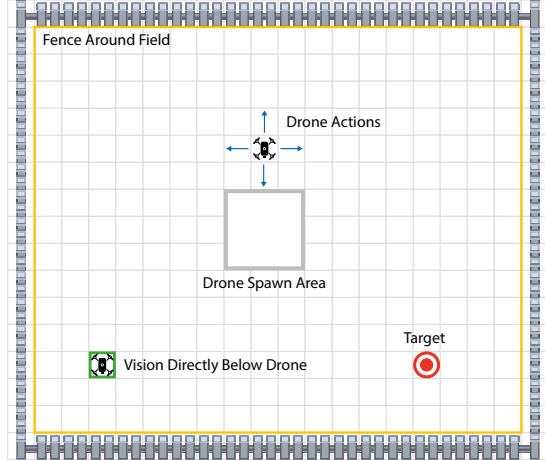


Figure 5: DroneScatter Environment

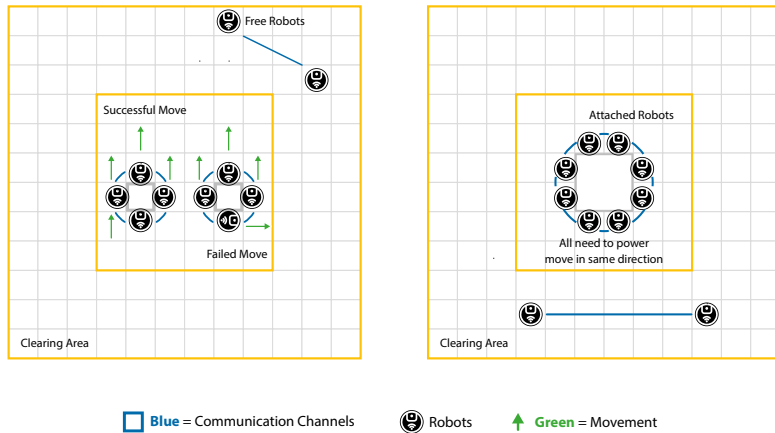


Figure 6: BoxPushing Environment

The **Box Pushing** environment is also a grid environment, which we design to test communication expressivity beyond 1-WL. It has 10 robots in a 12x12 construction site. The out-most 3 grid cells on every side represent the “clearing area”, into which robots need to clear the boxes from the central area of the site. Robots can see the cells next to them. Robots attach themselves to boxes before they can move them. When they are attached, robots cannot see around them any more. Free-roaming robots can communicate with any other free-roaming robots, but attached robots can only communicate with the robots directly adjacent to them. The environment either spawns with one large box or two small boxes. 4 attached robots are needed to move a small box. 8 attached robots are needed to move a large box. The agents have 9 possible actions: stay, move in 1 of the 4 cardinal directions, or power move in 1 of the 4 cardinal directions. A small box only moves if all attached agents move in the same direction. A large box only moves if all attached agents power move in the same direction. Robots are penalised for exerting themselves without moving the box, and are rewarded for moving the box closer to the clearing area or clearing the box. Once a box has been cleared, it is removed from the site and the agents are free to continue moving around the environment.

To solve the environment, the robots need to be able to communicate with each other to figure out which type of box they are on and all push correctly, at the same time, and in the same direction. Since the communication graphs corresponding to the scenarios with small and large boxes are 1-WL indistinguishable, communication beyond 1-WL is needed to properly solve the environment. In the “easy” version, robots spawn already attached to the boxes. The environment is demonstrated in Figure 6.

C.3 Hybrid Imitation Learning

We use hybrid imitation learning for all Box Pushing experiments to solve the issue of the exceptionally sparse rewards. Since agents are only given a reward when they all take the same action and thus move the box, random policies will struggle to ever obtain a meaningful reward signal during exploration. When agents are attached to a large box, the probability of this happening at a single time step is $4/9 \times (1/9)^7 = 9.29e-8$, meaning $\approx 10^8$ time steps of experience are needed before any reward can be expected.

Hester et al. [20] propose using expert demonstrations for training and Subramanian et al. [50] propose using some expert demonstrations to help exploration. Inspired by this, during training, we interleave 100 expert experiences for every 500 experiences collected by the agents in the environment. While this is stable for the value-based method DGN, doing so for the A2C methods leads to very unstable performance during training. Wang et al. [58] propose several ways to improve such training of A2C methods, but we choose not to implement them as it is not the focus of this paper.

C.4 Model and Environment Hyperparameters

C.4.1 Fixed Model Hyperparameters

Model hyperparameters that are fixed across all experiments are shown in Table 9, along with which group they belong to, their fixed values, and their descriptions.

C.4.2 TrafficJunction-Easy

Model hyperparameters for the Easy Traffic Junction experiments are shown in Table 10, along with which group they belong to, their values (sometimes a set of values), and their descriptions.

C.4.3 PredatorPrey

Model hyperparameters for the Predator-Prey experiments are shown in Table 11, along with which group they belong to, their values (sometimes a set of values), and their descriptions.

C.4.4 TrafficJunction-Medium

Model hyperparameters for the Medium Traffic Junction experiments are shown in Table 12, along with which group they belong to, their values (sometimes a set of values), and their descriptions.

C.4.5 BoxPushing

Model hyperparameters for the Box Pushing experiments are shown in Table 13, along with which group they belong to, their values (sometimes a set of values), and their descriptions.

C.4.6 DroneScatter-Stochastic

Model hyperparameters for the Drone Scatter experiments with stochastic evaluation are shown in Table 14, along with which group they belong to, their values (sometimes a set of values), and their descriptions.

C.4.7 DroneScatter-Greedy

Model hyperparameters for the Drone Scatter experiments with greedy evaluation are shown in Table 15, along with which group they belong to, their values (sometimes a set of values), and their descriptions.

Table 9: Fixed model parameters for all experiments

Group	Parameter	Value	Description
Training	epoch_size	10	Number of update iterations in an epoch
	batch_size	500	Number of steps before each update (per thread)
	nprocesses	1	How many processes to run
DGN Training	update_interval	5	How many episodes between model update steps
	train_steps	5	How many times to train the model in a training step
	dgn_batch_size	128	Batch size
	epsilon_start	1	Epsilon starting value
	epsilon_min	0.1	Minimum epsilon value
	buffer_capacity	40000	Capacity of the replay buffer
Model	hid_size	128	Hidden layer size
	qk_hid_size	16	Key and query size for soft attention
	value_hid_size	32	Value size for soft attention
	recurrent	True	Make the A2C model recurrent in time
	num_evals	10	Number of evaluation runs for each training iteration
	env_graph	True	Whether the environment masks communication
	comm_passes	4	Number of comm passes per step over the model
Optimization	gamma	1	Discount factor
	normalize_rewards	False	Normalize rewards in each batch
	lrate	0.001	Learning rate
	entr	0	Entropy regularization coefficient
	value_coeff	0.01	Coefficient for value loss term
A2C Models	comm_mode	avg	Mode for communication tensor calculation
	comm_mask_zero	False	Mask all communication
	mean_ratio	1	How much cooperation? 1 means fully cooperative
	rnn_type	MLP	Type of RNN to use [LSTM MLP]
	detach_gap	10	Detach hidden and cell states for RNNs at this interval
	comm_init	uniform	How to initialise comm weights [uniform zeros]
	hard_attn	False	Whether to use hard attention: action - talk silent
	comm_action_one	False	Whether to always talk
	advantages_per_action	False	Whether to multiply action log prob with advantages
	share_weights	True	Share model parameters between agents
MAGIC	directed	True	Whether the communication graph is directed
	self_loop_type	1	Self loop type in the GAT layers (1: with self loop)
	gat_num_heads	4	Number of heads in GAT layers except the last one
	gat_num_heads_out	1	Number of heads in output GAT layer
	gat_hid_size	32	Hidden size of one head in GAT
	message_decoder	True	Whether use the message decoder
	gat_normalize	False	Whether to normalize the GAT coefficients
	ge_num_heads	4	Number of heads in the GAT encoder
	gat_encoder_normalize	False	Normalize the coefficients in the GAT encoder
	use_gat_encoder	False	Whether use the GAT encoder
	gat_encoder_out_size	64	Hidden size of output of the GAT encoder
	graph_complete	False	Whether the communication graph is complete
	learn_different_graphs	False	Learn a new communication graph each round
	message_encoder	False	Whether to use the message encoder

Table 10: Hyperparameters for Easy Traffic Junction experiments

Group	Parameter	Value(s)	Description
Environment	difficulty	easy	Difficulty level [easy medium hard]
	dim	6	Dimension of box (i.e length of road)
	env_name	traffic_junction	Environment name
	max_steps	20	Force to end the game after this many steps
	nagents	5	Number of agents
	vision	1	Vision of car
	add_rate_min	0.3	Min probability to add car (till curr. start)
	add_rate_max	0.3	Max rate at which to add car
	curr_start	0	Start making harder after this epoch
	curr_end	0	When to make the game hardest
	vocab_type	bool	Type of location vector to use [bool scalar]
	comm_range	3	Agent communication range
Model	epsilon_step	2e-5	Amount to subtract from epsilon each episode
	model	[commnet, tarmac, ic3net, tarmac_ic3net, dgn, magic]	Which baseline model to use
	num_epochs	2000	Number of training epochs
	rni	[0.75, 0.25, 0, 1]	RNI ratio. 0 for none. 1 for unique IDs
	seed	[1, 2, 3, 4, 5]	Random seed

Table 11: Hyperparameters for Predator-Prey experiments

Group	Parameter	Value(s)	Description
Environment	dim	10	Dimension of box (i.e side length)
	env_name	predator_prey	Environment name
	max_steps	40	Force to end the game after this many steps
	mode	cooperative	Reward mode
	nagents	5	Number of agents
	vision	1	Vision of predator
	nenemies	1	Total number of preys in play
	moving_prey	False	Whether prey is fixed or moving
	no_stay	False	Whether predators have an action to stay
	comm_range	5	Agent communication range
	epsilon_step	2e-5	Amount to subtract from epsilon each episode
	model	[commnet, tarmac, ic3net, tarmac_ic3net, dgn, magic]	Which baseline model to use
Model	num_epochs	2000	Number of training epochs
	rni	[0.75, 0.25, 0, 1]	RNI ratio. 0 for none. 1 for unique IDs
	seed	[1, 2, 3, 4, 5]	Random seed

D Full Results

In this appendix, full results from all experiments are shown. Our experiments were done in parallel on an internal cluster, using only CPUs. With regards to compute time, 127 days were used for Easy Traffic Junction, 149 for Predator-Prey, 186 for Medium Traffic Junction, 502 for Box Pushing, 76 for stochastic Drone Scatter, and 89 for greedy Drone Scatter. This comes to a total of 1129 days.

D.1 Result Tables

In this section, scores for all metrics across all experiments are shown in Table 16 (Easy Traffic Junction), Table 17 (Predator-Prey), Table 18 (Medium Traffic Junction), Table 19 (Box Pushing), Table 20 (Drone Scatter with stochastic evaluation), and Table 21 (Drone Scatter with greedy evaluation).

Table 12: Hyperparameters for Medium Traffic Junction experiments

Group	Parameter	Value(s)	Description
Environment	difficulty	medium	Difficulty level [easy medium hard]
	dim	14	Dimension of box (i.e length of road)
	env_name	traffic_junction	Environment name
	max_steps	40	Force to end the game after this many steps
	nagents	10	Number of agents
	vision	1	Vision of car
	add_rate_min	0.3	Min probability to add car (till curr. start)
	add_rate_max	0.3	Max rate at which to add car
	curr_start	0	Start making harder after this epoch
	curr_end	0	When to make the game hardest
Model	vocab_type	bool	Type of location vector to use [bool scalar]
	comm_range	3	Agent communication range

Table 13: Hyperparameters for Box Pushing experiments

Group	Parameter	Value(s)	Description
Environment	difficulty	easy	Difficulty level. Easy: robots already attached
	dim	12	Dimension of area (i.e. side length)
	env_name	box_pushing	Environment name
	max_steps	20	Force to end the game after this many steps
	nagents	10	Number of agents
	vision	1	Vision of robot
Model	epsilon_step	2e-5	Amount to subtract from epsilon each episode
	imitation	True	Whether to use hybrid imitation learning
	model	[commnet, tarmac, ic3net, tarmac_ic3net, dgn, magic]	Which baseline model to use
	num_epochs	2000	Number of training epochs
	num_imitation_experiences	100	Number of experiences coming from imitation
	num_normal_experiences	500	Number of normal policy experiences
	rni	[0.75, 0.25, 0, 1]	RNI ratio. 0 for none. 1 for unique IDs
	seed	[1, 2, 3, 4, 5, 6, 7, 8, 9, 10]	Random seed

Table 14: Hyperparameters for Drone Scatter experiments with stochastic evaluation

Group	Parameter	Value(s)	Description
Environment	difficulty	easy	Difficulty level. Easy: rewarded for splitting
	dim	20	Dimension of field area (i.e. side length)
	env_name	drone_scatter	Environment name
	max_steps	20	Force to end the game after this many steps
	nagents	4	Number of agents
	comm_range	10	Agent communication range
	find_range	3	Agent distance to target to count as find
	min_target_distance	3	Min distance target can be from spawn area
Model	epsilon_step	2e-5	Amount to subtract from epsilon each episode
	model	[commnet, tarmac, ic3net, tarmac_ic3net, magic]	Which baseline model to use
	num_epochs	2000	Number of training epochs
	rni	[0.75, 0, 1]	RNI ratio. 0 for none. 1 for unique IDs
	seed	[1, 2, 3, 4, 5]	Random seed

Table 15: Hyperparameters for Drone Scatter experiments with greedy evaluation

Group	Parameter	Value(s)	Description
Environment	difficulty	easy	Difficulty level. Easy: rewarded for splitting
	dim	20	Dimension of field area (i.e. side length)
	env_name	drone_scatter	Environment name
	max_steps	20	Force to end the game after this many steps
	nagents	4	Number of agents
	comm_range	10	Agent communication range
	find_range	3	Agent distance to target to count as find
	min_target_distance	3	Min distance target can be from spawn area
Model	epsilon_step	2e-5	Amount to subtract from epsilon each episode
	greedy_a2c_eval	True	Whether to evaluate A2C methods greedily
	model	[commnet, tarmac, ic3net, tarmac_ic3net, dgn, magic]	Which baseline model to use
	num_epochs	2000	Number of training epochs
	rni	[0.75, 0, 1]	RNI ratio. 0 for none. 1 for unique IDs
	seed	[1, 2, 3, 4, 5]	Random seed

Table 16: Mean and 95% confidence interval for Easy TrafficJunction across all baselines

Baseline	Metric	Baseline	Unique IDs	0.75 RNI	0.25 RNI
CommNet	Success	1 ± 0	1 ± 0	1 ± 0	1 ± 0
	Reward	-1.7 ± 0.01	-1.69 ± 0	-1.78 ± 0.02	-1.7 ± 0.01
DGN	Success	0.987 ± 0	0.99 ± 0	0.848 ± 0.15	0.996 ± 0
	Reward	-4.48 ± 0.79	-4 ± 0.17	-9.35 ± 5.57	-3.99 ± 0.15
IC3Net	Success	1 ± 0	1 ± 0	1 ± 0	0.986 ± 0.02
	Reward	-1.71 ± 0	-1.7 ± 0.01	-1.74 ± 0.01	-2.02 ± 0.51
MAGIC	Success	0.634 ± 0.11	0.764 ± 0.13	0.684 ± 0.11	0.787 ± 0.09
	Reward	-16 ± 1.67	-15.8 ± 1.69	-15 ± 2.05	-14.7 ± 2.08
TarMAC	Success	0.994 ± 0.01	1 ± 0	0.933 ± 0.04	1 ± 0
	Reward	-2.07 ± 0.44	-1.72 ± 0.02	-3.59 ± 1.28	-1.76 ± 0.04
T-IC3Net	Success	1 ± 0	0.998 ± 0	0.94 ± 0.04	0.974 ± 0.04
	Reward	-1.74 ± 0.01	-1.79 ± 0.11	-3.16 ± 1.03	-2.25 ± 0.91

Table 17: Mean and 95% confidence interval for PredatorPrey across all baselines

Baseline	Metric	Baseline	Unique IDs	0.75 RNI	0.25 RNI
CommNet	Success	0.88 ± 0.03	0.908 ± 0.02	0.194 ± 0.02	0.476 ± 0.05
	Reward	23.15 ± 0.92	23.71 ± 1.18	1.828 ± 0.51	10.53 ± 1.92
DGN	Success	0.014 ± 0	0.016 ± 0	0.026 ± 0.03	0.032 ± 0.01
	Reward	-6.8 ± 0.71	-7.84 ± 0.26	-7.69 ± 0.91	-4.37 ± 2.63
IC3Net	Success	0.952 ± 0	0.93 ± 0.02	0.454 ± 0.08	0.933 ± 0.02
	Reward	22.54 ± 1.19	22.99 ± 0.52	10.19 ± 1.47	24.38 ± 1.63
MAGIC	Success	0.892 ± 0.02	0.888 ± 0.05	0.112 ± 0.03	0.451 ± 0.09
	Reward	21.62 ± 1.31	21.36 ± 1.65	-0.85 ± 1.63	9.487 ± 3.07
TarMAC	Success	0.169 ± 0.09	0.24 ± 0.11	0.068 ± 0.01	0.086 ± 0.02
	Reward	0.323 ± 3.65	3.131 ± 3.96	-5.22 ± 0.54	-3.14 ± 1.27
T-IC3Net	Success	0.938 ± 0.02	0.938 ± 0.01	0.27 ± 0.02	0.913 ± 0.02
	Reward	23.77 ± 1.03	23.24 ± 0.43	4.725 ± 0.97	22.79 ± 0.46

Table 18: Mean and 95% confidence interval for Medium TrafficJunction across all baselines

Baseline	Metric	Baseline	Unique IDs	0.75 RNI	0.25 RNI
CommNet	Success	0.761 ± 0.31	0.793 ± 0.33	0.046 ± 0	0.614 ± 0.11
	Reward	-50.4 ± 36	-68.9 ± 73.8	-168 ± 7.13	-48.5 ± 7.87
DGN	Success	1 ± 0	1 ± 0	0.062 ± 0	0.619 ± 0.4
	Reward	-62.7 ± 0.09	-62.7 ± 0.1	-245 ± 2.61	-138 ± 80.7
IC3Net	Success	0.971 ± 0.04	0.804 ± 0.1	0.588 ± 0.03	0.855 ± 0.13
	Reward	-22.6 ± 1.31	-28.1 ± 3.3	-42.2 ± 2.54	-27.1 ± 4.96
MAGIC	Success	0.551 ± 0.28	0.526 ± 0.33	0.734 ± 0.21	0.4 ± 0.35
	Reward	-132 ± 61.1	-112 ± 59.7	-173 ± 55.1	-198 ± 60.1
TarMAC	Success	0.064 ± 0	0.052 ± 0	0.05 ± 0	0.054 ± 0.01
	Reward	-187 ± 24.4	-182 ± 28.7	-245 ± 2.79	-211 ± 20.7
T-IC3Net	Success	0.89 ± 0.17	0.909 ± 0.08	0.362 ± 0.18	0.962 ± 0.02
	Reward	-26.4 ± 7.2	-24.9 ± 2.48	-94.2 ± 65.8	-23.7 ± 1.1

Table 19: Mean and 95% confidence interval for BoxPushing across all baselines

Baseline	Metric	Baseline	Unique IDs	0.75 RNI	0.25 RNI
CommNet	Ratio Cleared	0.786 ± 0.08	0.829 ± 0.08	0.768 ± 0.08	0.795 ± 0.09
	Reward	3777 ± 728	4439 ± 687	4313 ± 514	4196 ± 615
DGN	Ratio Cleared	0.603 ± 0	0.756 ± 0.06	0.958 ± 0	0.957 ± 0.01
	Reward	3811 ± 51.5	4127 ± 278	5536 ± 57	5469 ± 90.2
IC3Net	Ratio Cleared	0.49 ± 0.15	0.617 ± 0.14	0.34 ± 0.18	0.676 ± 0.06
	Reward	2528 ± 950	2990 ± 864	1341 ± 711	3306 ± 556
MAGIC	Ratio Cleared	0.958 ± 0.04	0.985 ± 0.01	0.975 ± 0.04	0.998 ± 0
	Reward	5199 ± 221	5322 ± 214	5444 ± 332	5464 ± 118
TarMAC	Ratio Cleared	0.629 ± 0.14	0.578 ± 0.11	0.662 ± 0.06	0.679 ± 0.06
	Reward	3425 ± 820	2961 ± 729	3343 ± 555	3610 ± 475
T-IC3Net	Ratio Cleared	0.558 ± 0.13	0.596 ± 0.11	0.458 ± 0.18	0.643 ± 0.15
	Reward	2979 ± 753	3062 ± 785	1917 ± 763	2908 ± 847

Table 20: Mean and 95% confidence interval for DroneScatter across all baselines except DGN, including a purely random agent. Stochastic evaluation

Baseline	Metric	Baseline	Unique IDs	0.75 RNI
CommNet	Pairwise Distance	11.34 \pm 0.9	12.08 \pm 1.12	8.687 \pm 1.4
	Steps Taken	11.5 \pm 0.26	9.767 \pm 0.32	11.74 \pm 1.39
	Reward	269 \pm 18.6	314.2 \pm 22	236 \pm 45.3
IC3Net	Pairwise Distance	9.108 \pm 1.45	13.3 \pm 0.71	10.99 \pm 0.38
	Steps Taken	11.94 \pm 0.84	10.13 \pm 0.25	11.66 \pm 0.22
	Reward	239.2 \pm 33.7	316.7 \pm 11.3	260.9 \pm 8.62
MAGIC	Pairwise Distance	7.693 \pm 1.47	12.59 \pm 1	7.216 \pm 0.76
	Steps Taken	13.05 \pm 0.58	11.12 \pm 1.05	13.54 \pm 0.21
	Reward	205.6 \pm 21.4	273.9 \pm 36.7	180 \pm 17.3
TarMAC	Pairwise Distance	7.448 \pm 0.89	10.26 \pm 0.69	8.486 \pm 0.36
	Steps Taken	13.49 \pm 0.1	10.7 \pm 0.35	12.85 \pm 0.57
	Reward	171.4 \pm 13.8	270.4 \pm 7.81	200.2 \pm 14.8
T-IC3Net	Pairwise Distance	8.891 \pm 0.27	12.9 \pm 0.78	9.552 \pm 0.57
	Steps Taken	12.28 \pm 0.6	10.33 \pm 0.46	12.22 \pm 0.82
	Reward	219 \pm 37.2	309 \pm 12	224.9 \pm 22.5
Random	Pairwise Distance	5.8 \pm 0.02	—	—
	Steps Taken	17.39 \pm 0.04	—	—
	Reward	44.59 \pm 1.73	—	—

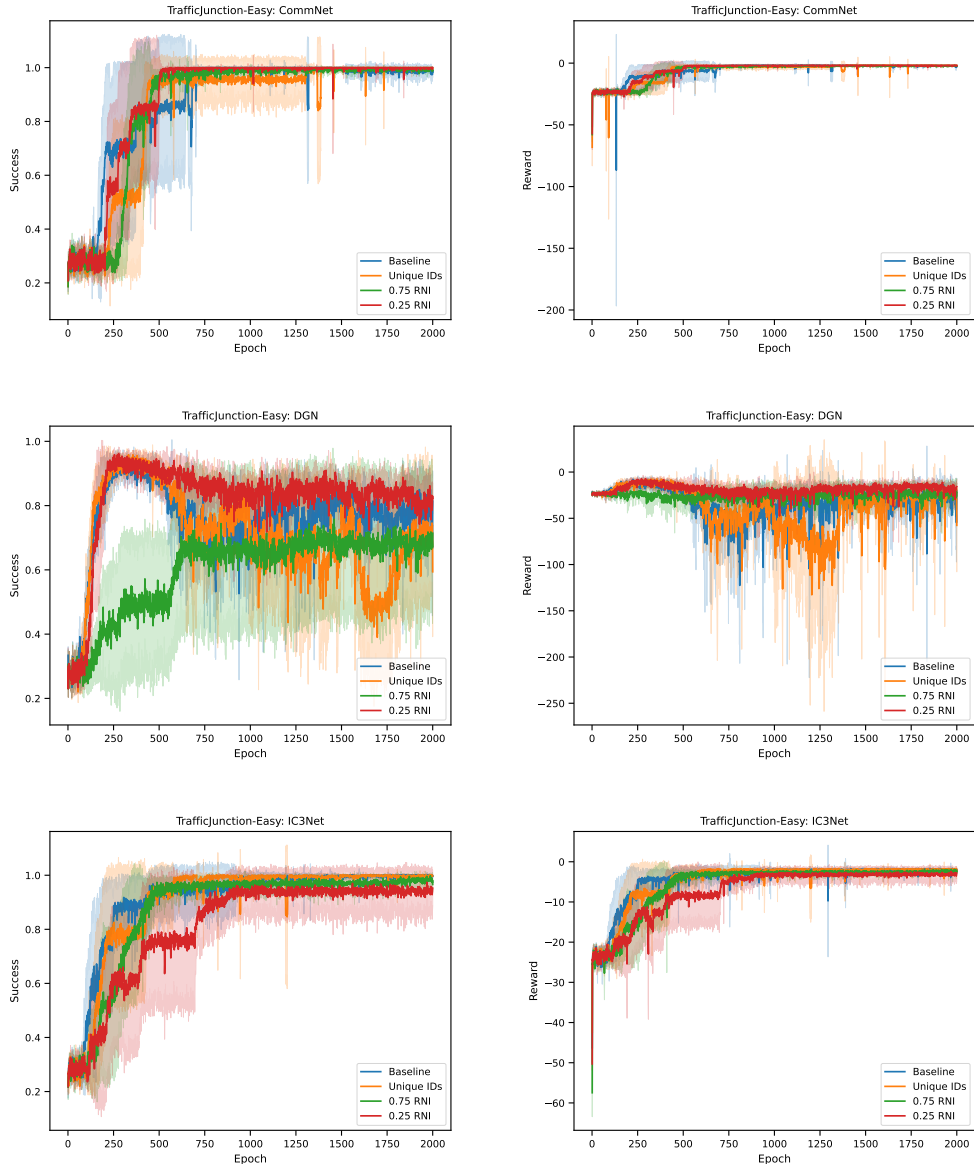
Table 21: Mean and 95% confidence interval for DroneScatter across all baselines. Greedy evaluation

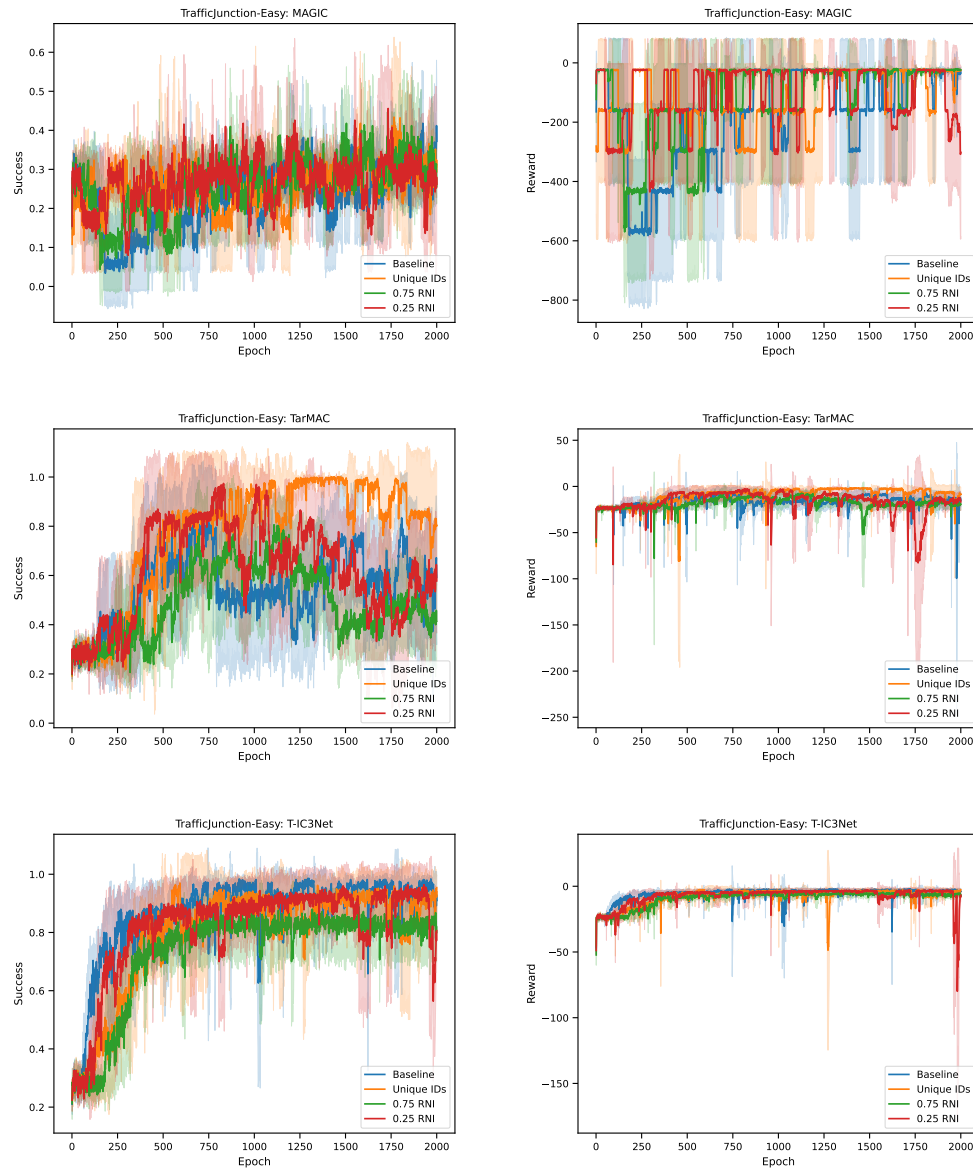
Baseline	Metric	Baseline	Unique IDs	0.75 RNI
CommNet	Pairwise Distance	8.849 \pm 0.63	13.28 \pm 1.27	8.589 \pm 1.35
	Steps Taken	13.79 \pm 0.12	9.554 \pm 0.33	12.62 \pm 1.19
	Reward	170.6 \pm 6.72	319.7 \pm 24.7	204.8 \pm 40.5
DGN	Pairwise Distance	3.221 \pm 0.18	4.427 \pm 0.67	3.706 \pm 0.83
	Steps Taken	13.36 \pm 0.15	13.27 \pm 0.21	13.46 \pm 0.14
	Reward	147.9 \pm 6.16	154.4 \pm 6.63	149.3 \pm 5.38
IC3Net	Pairwise Distance	7.69 \pm 1.03	14.09 \pm 0.54	11 \pm 0.86
	Steps Taken	13.25 \pm 0.4	10.14 \pm 0.2	11.42 \pm 0.48
	Reward	186.6 \pm 8.87	310.1 \pm 11	264.3 \pm 21.9
MAGIC	Pairwise Distance	6.61 \pm 1.28	12.58 \pm 0.6	7.107 \pm 1.59
	Steps Taken	13.27 \pm 0.18	11.84 \pm 0.68	13.61 \pm 0.25
	Reward	193.3 \pm 15.2	222.7 \pm 26.6	161.3 \pm 23.9
TarMAC	Pairwise Distance	8.666 \pm 0.28	12.09 \pm 0.73	8.999 \pm 0.94
	Steps Taken	13.73 \pm 0.21	11.01 \pm 0.86	12.19 \pm 0.82
	Reward	139.1 \pm 4.43	255.5 \pm 31.4	202.9 \pm 32.6
T-IC3Net	Pairwise Distance	7.28 \pm 0.69	13.51 \pm 0.98	10.87 \pm 1.17
	Steps Taken	13.96 \pm 0.26	10.63 \pm 0.66	11.73 \pm 0.54
	Reward	156.9 \pm 21.9	278.6 \pm 32.1	240.3 \pm 25.6

D.2 Result Plots

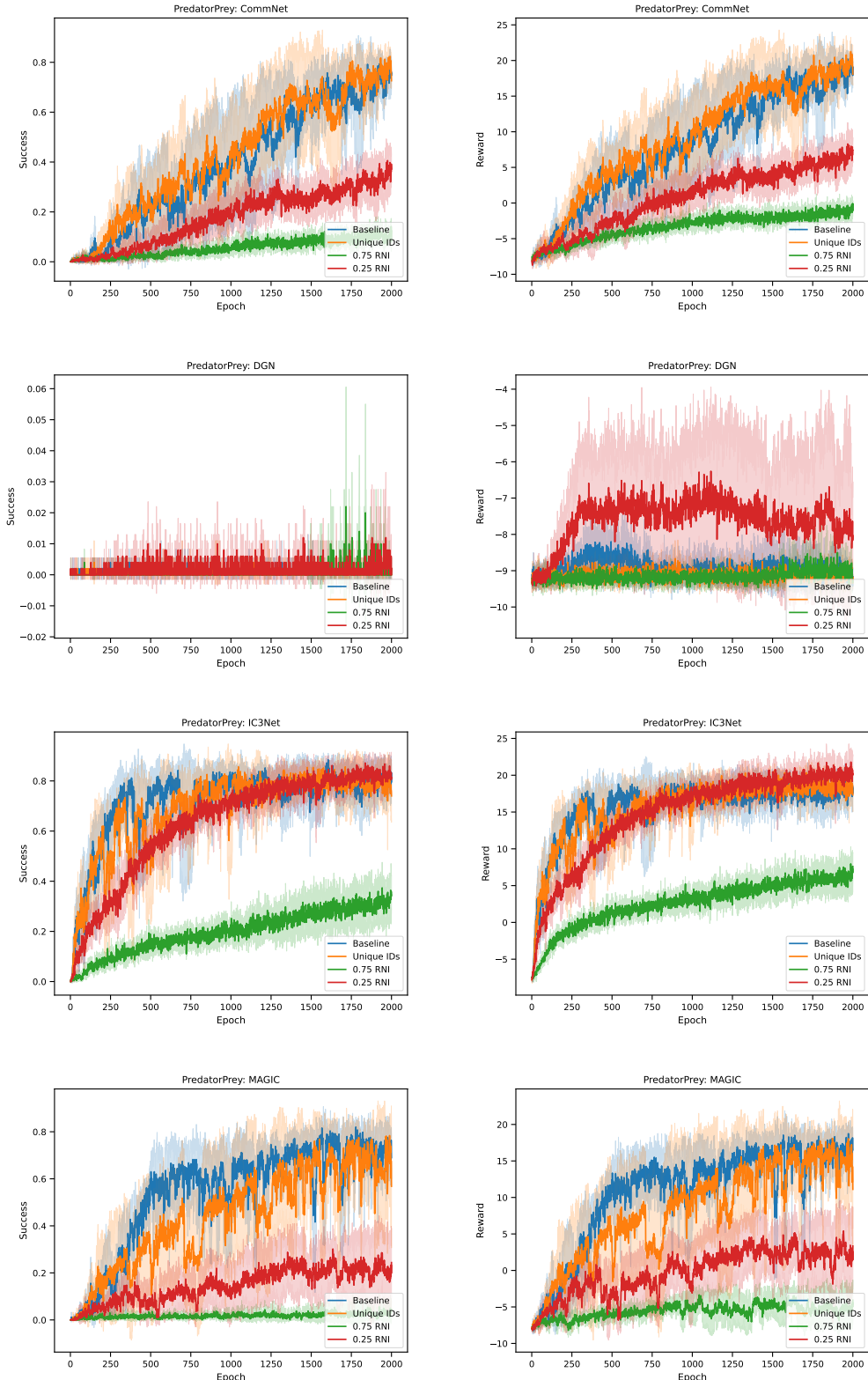
In this section, we provide the full result plots for all of our experiments. For all but the BoxPushing experiments, results are shown aggregated across 5 seeds, with a 95% confidence interval. For the BoxPushing experiments, the hybrid imitation learning paradigm yielded unstable training for all A2C methods. Thus, to better visualize the results, for each seed, we first denote the performance at each epoch to be the maximum performance achieved so far. Then, we aggregate these runs across 10 seeds, showing the mean and a 95% confidence interval.

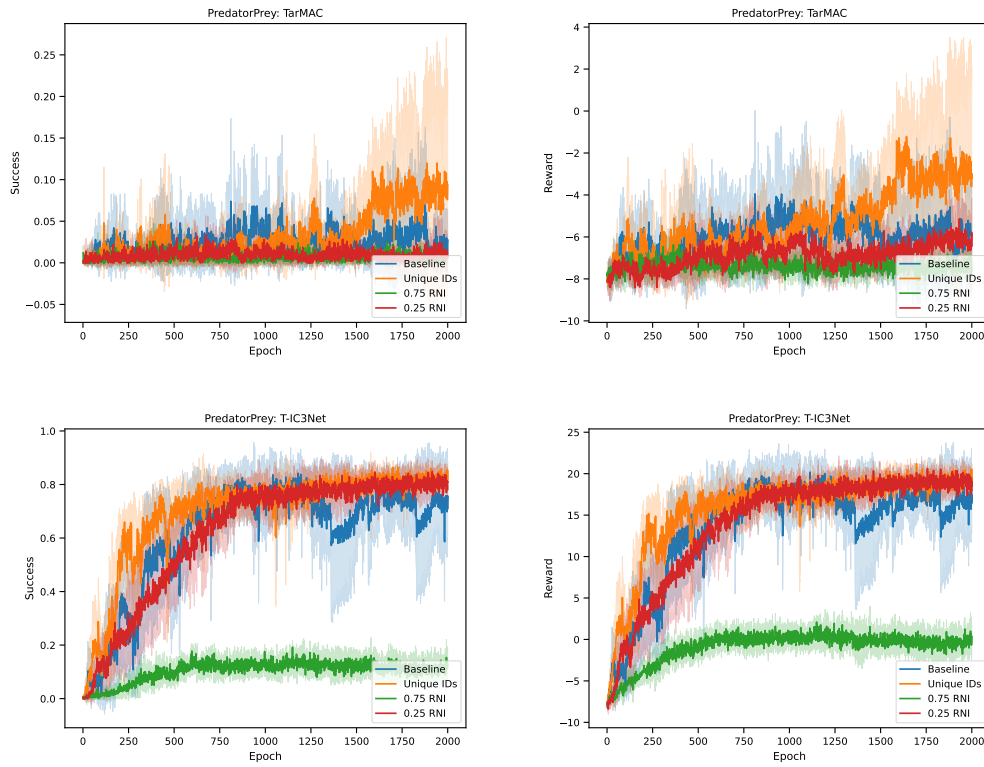
D.3 TrafficJunction-Easy



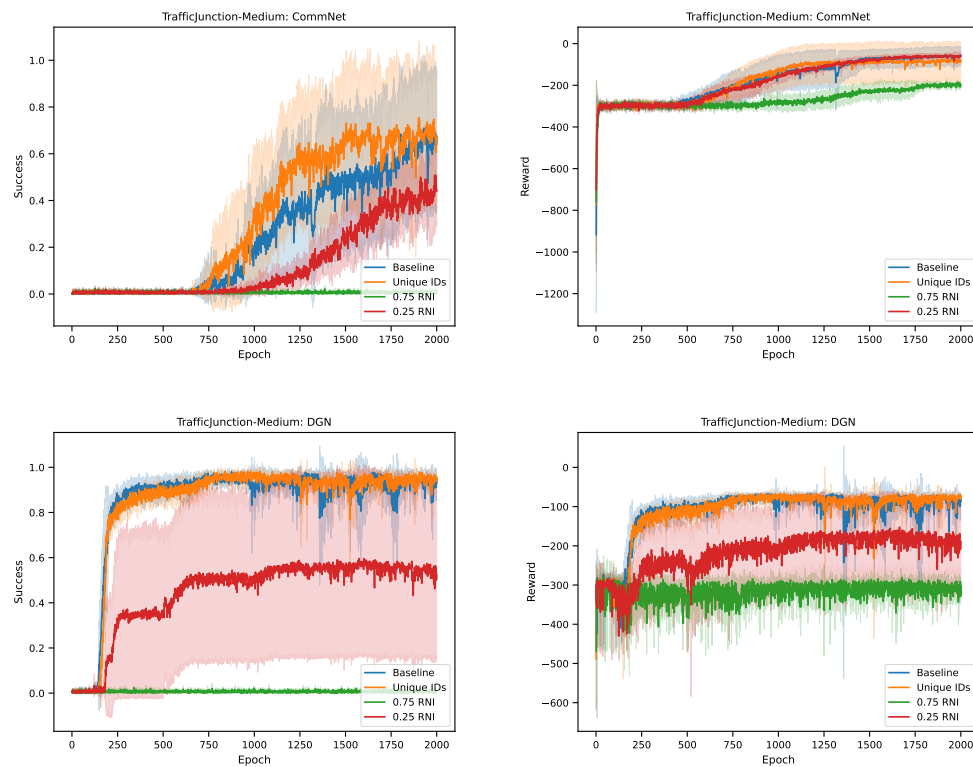


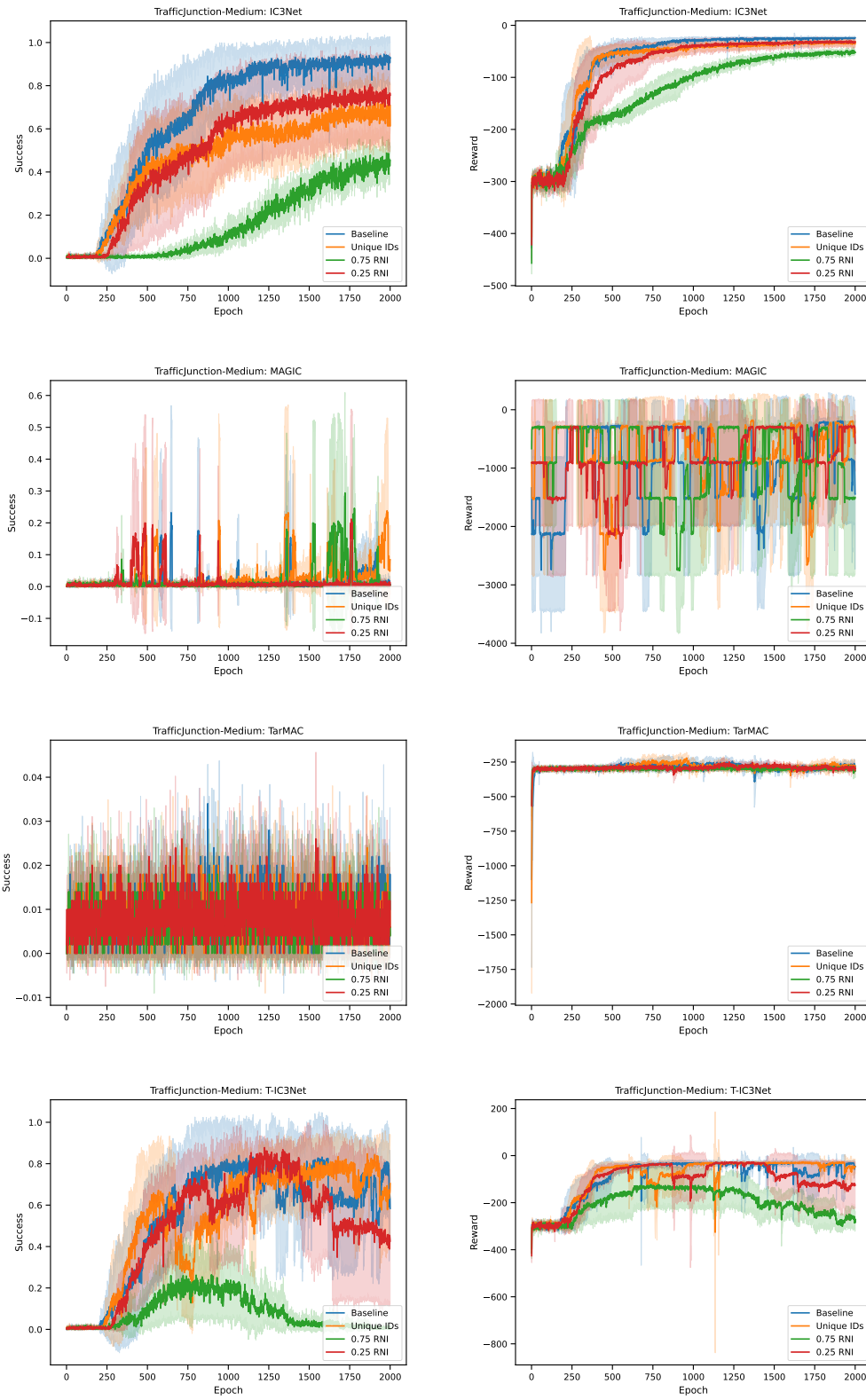
D.4 PredatorPrey



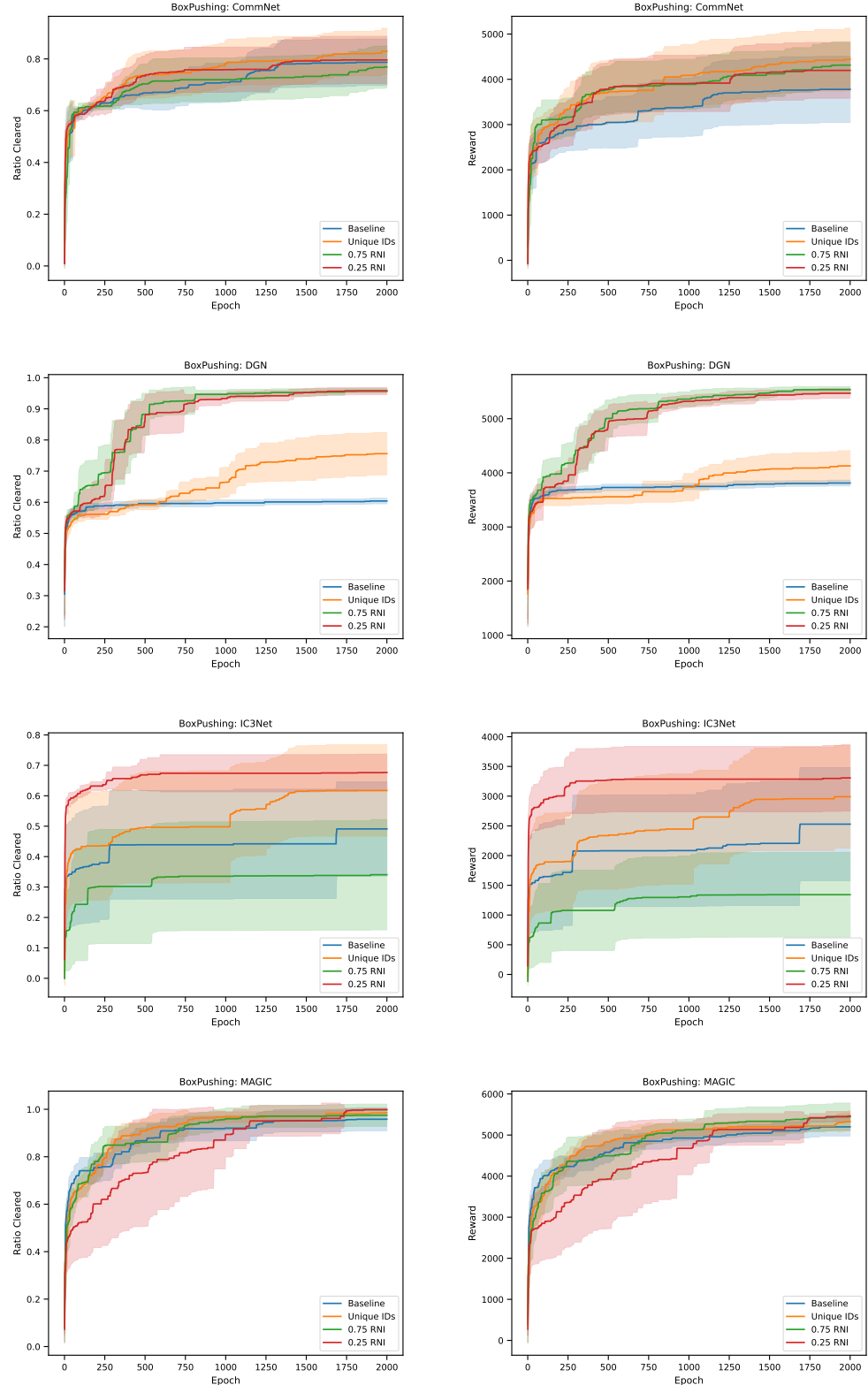


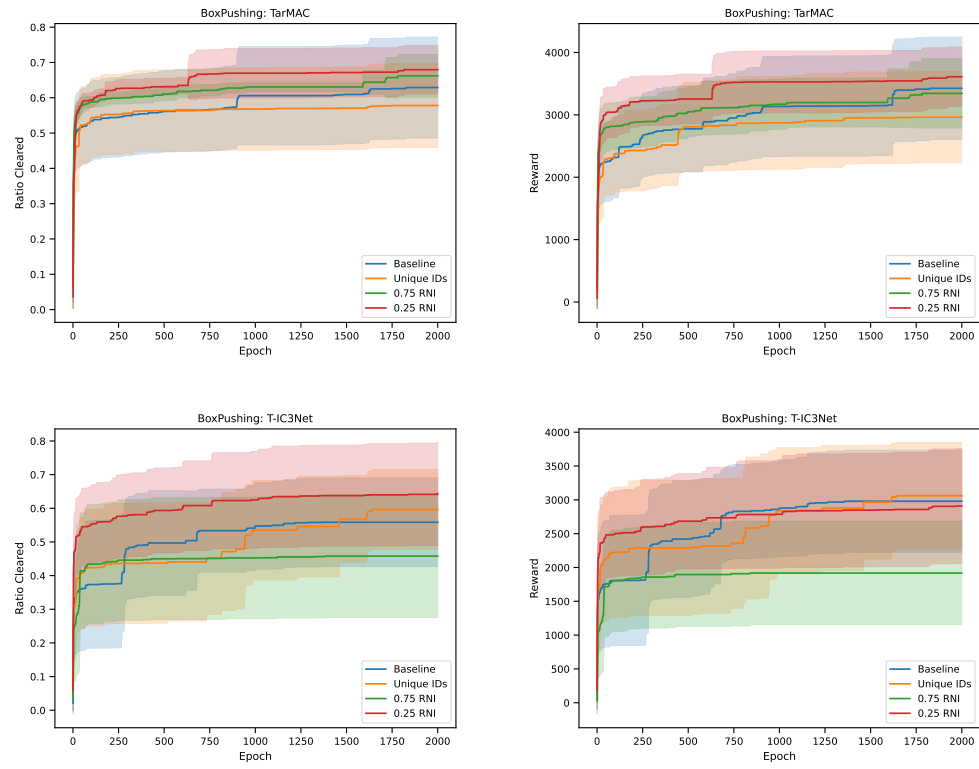
D.5 TrafficJunction-Medium



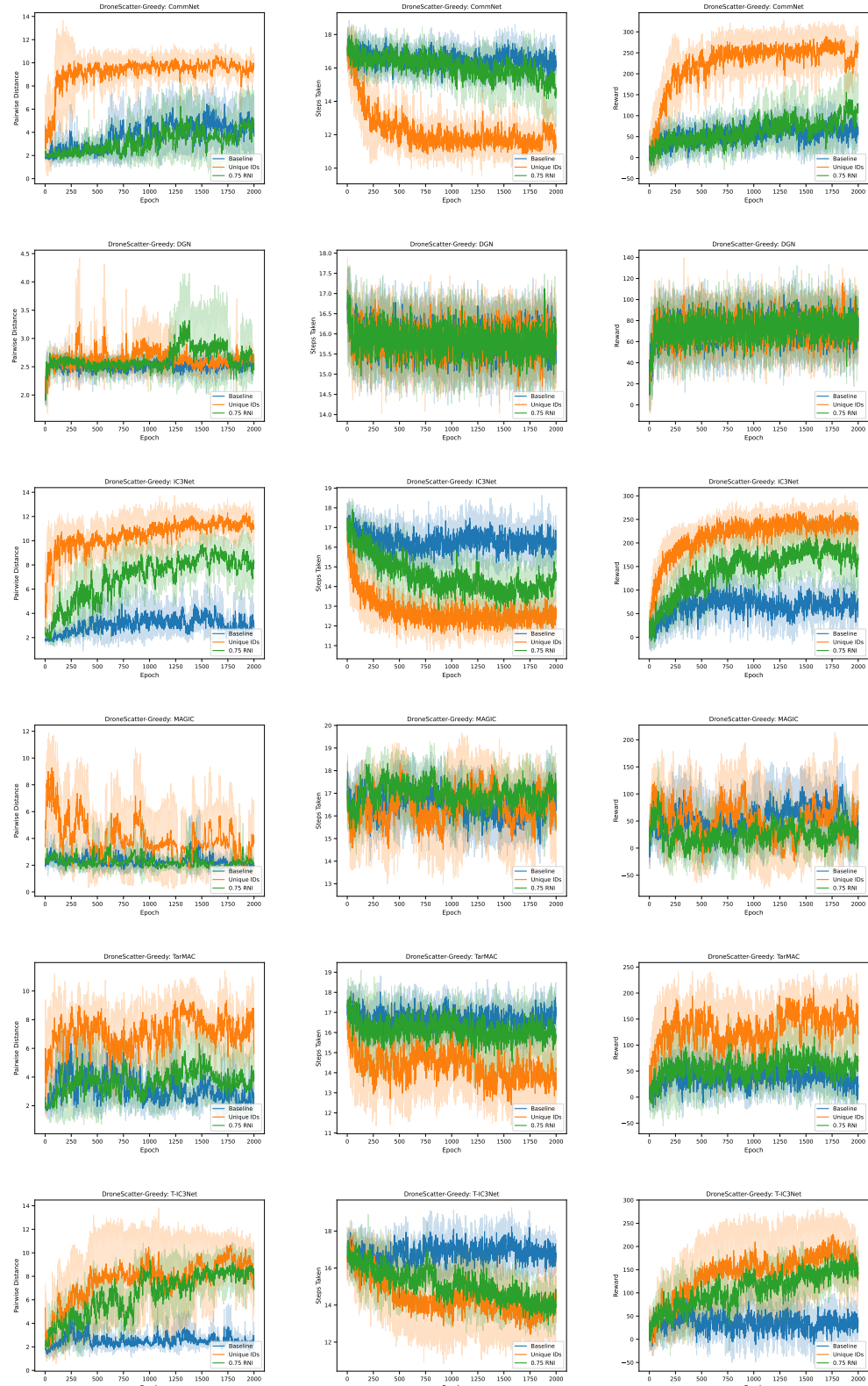


D.6 BoxPushing





D.7 DroneScatter with Greedy Evaluation



D.8 DroneScatter with Stochastic Evaluation

